Establishment of a Stable Human Cell Line, HPL-A3, for Use in Reporter Gene Assays of Cytochrome P450 3A Inducers

Masashi Sekimoto, Shinsuke Sano,† Takuomi Hosaka,‡ Kiyomitsu Nemoto, and Masakuni Degawa*

Department of Molecular Toxicology and Global Center of Excellence Program, School of Pharmaceutical Sciences, University of Shizuoka; 52–1 Yada, Suruga-ku, Shizuoka 422–8526, Japan.
Received November 4, 2011; accepted February 22, 2012; published online March 5, 2012

We have established a stable human cell line, termed HPL-A3, by co-transfection of a human pregnane X receptor (hPXR) expression vector and a reporter plasmid (p3A4-hPXRE-Luc) containing a luciferase gene and a promoter/enhancer region of the human *cytochrome P450 3A4* (*CYP3A4*) gene into a human hepatoma-derived cell line, HepG2. We then examined the usefulness of HPL-A3 for a chemically activated luciferase expression (CALUX) assay of human CYP3A inducers. The induction of CALUX in HPL-A3 by hPXR activators, including rifampicin, occurred in time- and concentration-dependent fashions, whereas no such induction was observed using rat/mouse PXR activators, such as pregnenolone-16α-carbonitrile and dexamethasone. The hPXR activator-mediated induction of CYP3As, especially CYP3A4, was observed at levels of both mRNA and enzyme activity. Furthermore, there were positive correlations between chemical-mediated inductions of CALUX and CYP3A4 mRNA levels. In addition, the induction of CALUX by dihydropyridine calcium channel blockers, which are known to act as CYP3A inducers in rats, was observed in HPL-A3 cells. Interestingly, expression levels of not only hPXR but also of vitamin D receptor (VDR), a transcription factor that positively regulates CYP3A subfamily genes, were significantly increased in HPL-A3 cells compared with those in the parental cell line, HepG2. Consequently, VDR ligand (1,25-dihydroxyvitamin D_3)-mediated inductions of CALUX and CYP3A4 mRNA were observed in the cells. These findings verified the usefulness of HPL-A3 for the screening of CYP3A inducers, which can activate the hPXR and/or hVDR.

Key words cytochrome P450 3A4; pregnane X receptor; vitamin D receptor; chemically activated luciferase expression; calcium channel blocker

Human cytochrome P450 3A (CYP3A) subfamily enzymes, especially CYP3A4, play important roles in the metabolism of xenobiotics, including drugs, agricultural chemicals and endocrine disrupters.[1,2] Accordingly, studies on xenobiotic-mediated induction/inhibition of CYP3A enzymes are important for understanding the therapeutic/toxic effects of xenobiotics, including drugs. We can now assess the inhibitory effects of xenobiotics on the activity of human CYP3A enzymes by *in vitro* assays using commercially available human hepatic microsomes and/or enzymes.[3] However, only a few *in vitro* induction assays are established, because there are only a limited number of cell lines capable of xenobiotic-mediated induction of CYP3A enzymes.[4] The lack of such responsiveness of cultured cell lines to xenobiotics is caused by a considerable decrease in the expression level of pregnane X receptor (PXR),[5] a main transcription factor for the *CYP3A* subfamily genes.[6,7] Likewise, vitamin D receptor (VDR)[8] and constitutive androstane receptor (CAR),[9] which also act as a transcriptional activators of *CYP3A* subfamily genes, are expressed at low levels or not at all in human hepatoma-derived cell lines, including HepG2.[5,10]

Recently, several stable cell lines for a human PXR (hPXR)-based reporter gene assay for the screening of CYP3A4 inducers have been established by co-transfection into human cell lines of an hPXR expression vector and a plasmid containing a reporter gene and hPXR-binding elements.[11–15] However, the available data on the xenobiotic-mediated induction of CYP3A enzymes at the levels of mRNA and activity in the reported cell lines are limited.

In the present study, to further develop an improved tool for the assessment of human CYP3A inducers, we have established a human cell line applicable for not only the reporter gene assay but also for assays of mRNA levels and enzyme activities. We confirmed the usefulness of the established cell line, termed HPL-A3, in assays of human CYP3A inducers.

MATERIALS AND METHODS

Chemicals Rifampicin (RIF), clotrimazole (CLO), pregnenolone-16α-carbonitrile (PCN), dexamethasone (DEX), tamoxifen citrate (TAM), nimodipine (NIM) and 1,25-dihydroxyvitamine D_3 (VD_3) were purchased from Sigma Chemical Co. (St. Louis, MO, U.S.A.). Nicardipine hydrochloride (NIC), nifedipine (NIF), nisoldipine (NIS), nitrendipine (NIT), and dimethylsulfoxide (DMSO) were obtained from Wako Pure Chemical (Osaka, Japan). The structures of chemicals used in this study are shown in Fig. 1. All the chemicals examined were dissolved in DMSO.

Construction of Reporter Plasmid The nuclear hormone receptor binding motif (ER6, −172 to −149) and distal nuclear receptor (dNR)-binding elements, such as dNR-1 (−7733 to −7719) and dNR-2 (−7489 to −7472), in a promoter/enhancer region of the human *CYP3A4* gene play a crucial role in the PXR-mediated induction of the gene.[16] Therefore, an hPXR reporter plasmid, termed p3A4-hPXRE-Luc, containing a

†Present address: *Department of Hospital Pharmacy, Hamamatsu University School of Medicine; 1–20–1 Handayama, Higashi-ku, Hamamatsu, Shizuoka 431–3192, Japan.*

‡Present address: *Department of Toxicology, Faculty of Pharmaceutical Sciences, Setsunan University; 45–1 Nagaotouge-cho, Hirakata, Osaka 573–0101, Japan.*

* To whom correspondence should be addressed. e-mail: degawa@u-shizuoka-ken.ac.jp

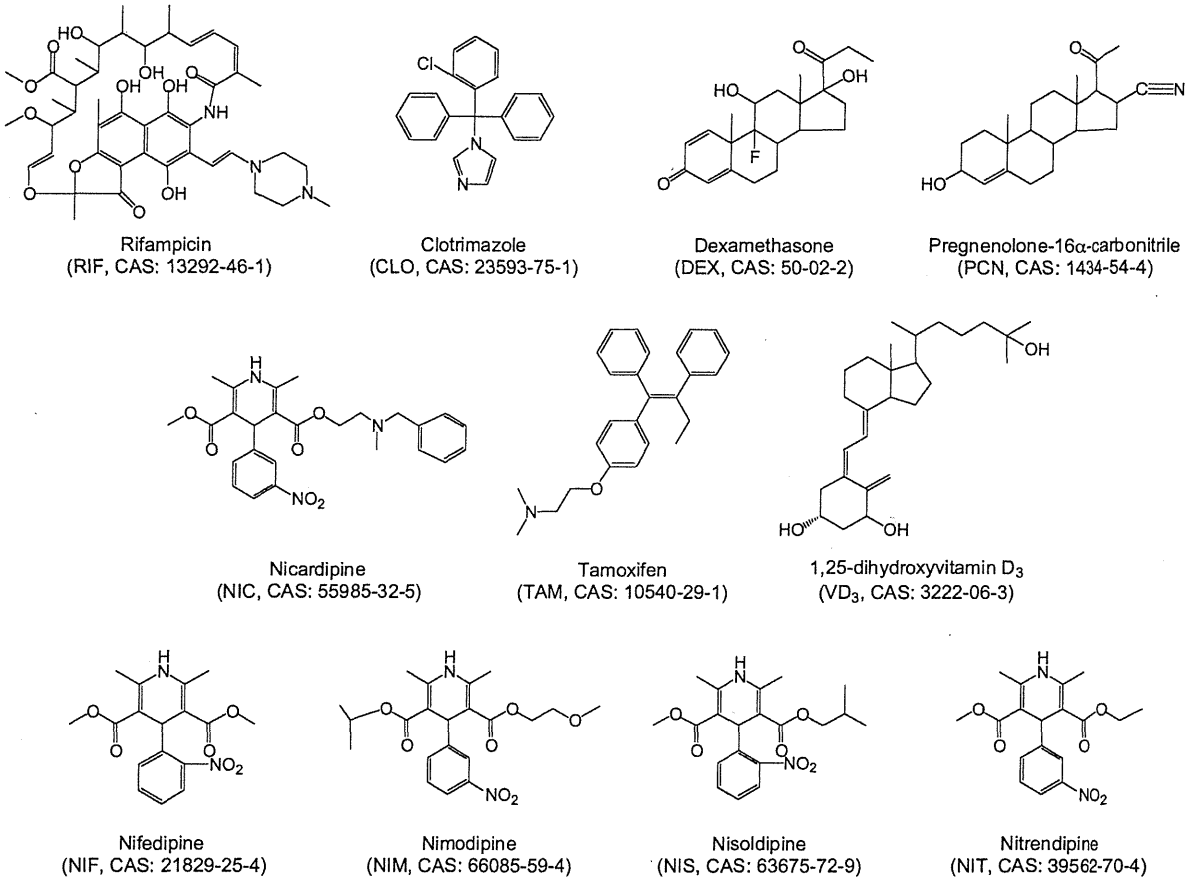

Fig. 1. Structures of Chemicals Used in This Study

luciferase gene and the promoter region (−362 to +53) and enhancer region (−7839 to −7208) of human *CYP3A4* gene was prepared using a previously reported method[16] with slight modifications.

In this study, human genomic DNA (Batch number; M00021571, Novagen, WI, U.S.A.) was used as a template for the amplification of the promoter/enhancer regions by polymerase chain reaction (PCR). A luciferase reporter plasmid, p3A4-hPXRE-Luc, was constructed through five steps as follows: (1) The promoter fragment A (−362 to +53) containing an ER-6 motif was prepared by *Bgl*II and *Bam*HI digestion of the promoter region (−1084 to +53), which was amplified by PCR with a primer set: forward sequence (bases −1085 to −1065, 5′-TCA TTG CTG GCT GAG GTG GTT-3′) and reverse sequence (bases +29 to +53, 5′-CAT GGA TCC TGT TGC TCT TTG CTG GGC TAT GTG C-3′), which has an engineered *Bam*HI digestion site, (2) The plasmid (p3A4-Luc) was constructed by insertion of the promoter fragment A into the *Bgl*II site of the PicaGene Basic Vector 2 (pGV-B2, NipponGene, Tokyo, Japan), (3) The enhancer fragment B (−7836 to −7208) containing dNR-1 and dNR-2 was prepared by PCR with a primer set: forward sequence (bases −7839 to −7810, 5′-GAA GAT CTA TTC TAG AGA GAT GGT TCA TTC CTT TCA-3′), which has an engineered *Bgl*II digestion site, and reverse sequence (bases −7208 to −7235, 5′-TCT CGT CAA CAG GTT AAA GGA GAA TGG T-3′), (4) The plasmid (hPXRE-pGEM-T) was prepared by insertion of the enhancer fragment B into the pGEM-T easy vector (Promega, Madison, MI, U.S.A.) containing a *Bam*HI site by the TA-cloning method, and (5) p3A4-hPXRE-Luc was prepared by insertion of the *Bam*HI–*Bgl*II digested hPXRE-pGEM-T fragment, containing enhancer fragment B, into the *Bgl*II site of p3A4-Luc. The obtained p3A4-hPXRE-Luc plasmid was used for the establishment of the cell line applicable to the hPXR-based chemically activated luciferase expression (CALUX) assay.

Construction of hPXR Expression Plasmid The full-length coding region of the human *PXR* gene was amplified from cDNA of a human hepatocellular carcinoma cell line, HepG2, by PCR with a primer set: forward sequence, 5′-GCC GCC ACC ATG GAG GTG AGA CCC AAA GAA AGC-3′; reverse sequence, 5′-AGC CGC TCA GCT ACC TGT GAT GCC GAA CAA-3′. An hPXR expression plasmid was prepared by the insertion of the full-length hPXR cDNA into the pTARGET Mammalian Expression vector (Promega) according to the manufacturer's instructions.

Establishment of a Cell Line for the hPXR-Based Reporter Gene Assay The reporter plasmid, p3A4-hPXRE-Luc, and the hPXR expression plasmid were co-transfected into HepG2 cells using Lipofectamine reagent (Life Technologies, Carlsbad, CA, U.S.A.) in Opti-MEM-I Reduced Serum Media (Life Technologies) for 24 h. After the co-transfection, a portion (10^4 cells/10 mL culture medium) of cell suspension was seeded in 100-mm culture dishes (Corning, Corning, NY, U.S.A.) and then cultured in Dulbecco's modified Eagle's medium (DMEM, Nissui, Tokyo, Japan) supplemented with 5% fetal calf serum and G418 (400 μg/mL medium) for

2 weeks. The G418-resistant cells were selected and further cloned. Consequently, eight clones (HPLs-A3, A7, A11, A12, A13, A14, A17 and A18) expressing hPXR and luciferase were obtained.

Luciferase Assay Luciferase assays were performed as previously described.[17,18] In brief, each HPL clone (5×10^4 cells/well) was pre-cultured for 48 h in a 24-well plate (Corning) and further incubated for the indicated times after addition of each test chemical to the culture medium. After incubation, cells were treated with 100 μL of 1×Reporter Lysis Buffer (Promega) for 15 min at room temperature, frozen at −80°C for 30 min and defrosted at room temperature. A portion (10 μL) of the resultant cell lysates was mixed with 50 μL of PicaGene Luminescence Reagent (Toyo-INK, Tokyo, Japan), and the amount of the luminescence product formed was immediately measured with a Luminescencer-PSN (ATTO, Tokyo, Japan). The amount of protein in cell lysates was measured using a bicinchoninic acid (BCA)-protein Assay Kit (Thermo Fisher Scientific, Rockford, IL, U.S.A.). Luciferase activity was represented as a luminescence unit per mg protein.

Clone HPL-A3 showed the greatest ability to induce chemical-mediated luciferase activity among the clones examined. Therefore, HPL-A3 was used for further experiments.

Gene Expression of CYP3A4 and Its Positive Transcriptional Regulators Constitutive gene expression levels of the positive transcriptional nuclear receptors (PXR, VDR, and CAR) of the *CYP3A4* gene and of their partner protein, retinoid X receptor α (RXRα), were determined by reverse transcription (RT)-PCR method[17,18] with the appropriate primer

Table 1. The Primer Sets and Amplification Protocols Used in This Study

Target gene	Primer set	Reaction condition			Cycle	Reference
		Denaturation	Annealing	Elongation		
Conventional PCR						
PXR	5′-TTG TTC GGC ATC ACA GGT AG-3′ (forward)	95°C, 30 s	60°C, 30 s	72°C, 60 s	25	(19)
	5′-CTT GCC TCT CTG ATG GTC CT-3′ (reverse)					
CAR	5′-GCA GCT GTG GAA ATC TGT CA-3′ (forward)	95°C, 30 s	60°C, 30 s	72°C, 60 s	35	(20)
	5′-CAG GTC GGT CAG GAG AGA AG-3′ (reverse)					
VDR	5′-CTC TTC AGA CAT GAT GGA CTC G-3′ (forward)	95°C, 30 s	60°C, 30 s	72°C, 60 s	28	(21)
	5′-GGA TGC TGT AAC TGA CCA GG-3′ (reverse)					
RXRα	5′-AGC TTG TGT CCA AGA TGC G-3′ (forward)	95°C, 30 s	60°C, 30 s	72°C, 60 s	25	(21)
	5′-ACT TGT GCT TGC AGT AGG CC-3′ (reverse)					
GAPDH	5′-TGT TGC CAT CAA TGA CCC CTT-3′ (forward)	95°C, 30 s	60°C, 30 s	72°C, 60 s	18	(22)
	5′-AGC ATC GCC CCA CTT GAT TTT G-3′ (reverse)					
Real-time PCR						
CYP3A4	5′-ATA AGT AAG GAA AGT AGT GAT GGC TCT CA-3′ (forward)	95°C, 30 s	60°C, 30 s	72°C, 60 s	40	(23)
	5′-TCA AAC ATA CAA AAG CCC TTA TGG TA-3′ (reverse)					
GAPDH	5′-TGT TGC CAT CAA TGA CCC CTT-3′ (forward)	95°C, 30 s	60°C, 30 s	72°C, 60 s	40	(22)
	5′-AGC ATC GCC CCA CTT GAT TTT G-3′ (reverse)					

sets.[19–23] The primer sets and amplification protocol used are shown in Table 1.

In brief, HPL-A3 or its parent cell line, HepG2, was cultured for 48 h in a 60-mm dish (Corning) (5×10^5 cells/dish). Total RNA was then isolated from the cells using Isogen (NipponGene). A portion (4 μg) of the prepared total RNA was converted to cDNA in an RT-reaction mixture (20 μL) containing Moloney Murine Leukemia Virus Reverse Transcriptase (Life Technologies) and Random Hexamers (Life Technologies). PCR was performed in a reaction mixture (25 μL) containing the prepared cDNA (equivalent to 32 ng of total RNA), the corresponding primer sets (each 12.5 pmol), and AmpliTaq Gold (0.625 units, Life Technologies) with a GeneAmp PCR system model 9600 (Life Technologies). The PCR products were separated by electrophoresis on a 2% agarose gel and visualized by ethidium bromide staining under UV light.

To determine chemical-altered *CYP3A4* expression, real-time PCR analysis was performed using an Applied Biosystems 7300 (Life Technologies) in 25 μL of reaction mixture containing the prepared cDNA (equivalent to 32 ng of total RNA), 12.5 μL of the Power SYBR Green PCR Master Mix (Life Technologies), the corresponding primer sets (each 12.5 pmol). After the reaction, dissociation curve analysis was carried out to confirm the amplification of a single PCR product. The amounts of CYP3A4 and glyceraldehyde-3-phosphate dehydrogenase (GAPDH) mRNAs were assessed by the relative standard curve method. *CYP3A4* and *GAPDH* fragments, obtained by conventional PCR with the corresponding primer sets (Table 1), were purified using a Qiaquick PCR Purification Kit (QIAEN, Valencia, CA, U.S.A.) and used as standard cDNAs. The level of CYP3A4 mRNA was normalized to that of GAPDH, an internal control.

Chemical-Mediated Induction of CYP3A Enzyme Activity The total activity of CYP3A subfamily enzymes was determined using a P450-Glo™ CYP3A4 Biochemical and Cell-Based Assay (Promega), as described in the instruction manual. In brief, HPL-A3 cells (10^4 cells/well) were pre-cultured for 48 h in a 96-well plate (Corning) and further treated with a chemical for the indicated times. After chemical treatment, cells were cultured for 4 h in serum-free DMEM containing Luciferin-PFBE (50 μM), a substrate of CYP3A subfamily enzymes (including CYP3A4, CYP3A5, and CYP3A7).[24] Thereafter, a portion (50 μL) of the culture supernatant was mixed with an equal volume of Luciferin Detection Reagent, and the mixture was incubated at room temperature for 20 min under light shielding. The amount of luciferin formed was measured using a Luminescencer-PSN. In addition, the protein contents of cell lysates were measured with a BCA-protein Assay Kit. The CYP3A enzyme activity was represented as a luminescence unit per mg protein.

Statistics Statistically significant differences between control group (treatment with a vehicle alone) and each chemical-treated group were assessed using Student's *t*-test. Time- and concentration-dependent effects were analyzed using one-way analysis of variance (ANOVA) and Dunnett's *post hoc* test. Furthermore, the correlation between two parameters was evaluated by regression analysis. These analyses were performed using ystat2002, a Microsoft Excel-based Statistical Program (Igaku Tosho Shuppan, Tokyo, Japan).

RESULTS

Selection of a Stable Cell Clone Applicable to hPXR-Based CALUX Assays G418-resistant cells were selected from HepG2 cells co-transfected with the reporter plasmid, p3A4-hPXRE-Luc, and the hPXR expression vector and further cloned. From 19 G418-resistant clones obtained, eight clones (HPLs-A3, A7, A11, A12, A13, A14, A17 and A18) that stably expressed luciferase were selected using the CALUX assay with RIF (10 μM), a representative hPXR activator. The concentration of RIF used was determined on the basis of previously reported data.[12,14] Clone HPL-A3 showed the greatest response to the RIF-mediated CALUX induction among the eight clones examined, although the other clones examined, with the exception of two clones (HPL-A14 and HPL-A18), showed moderate responses (Table 2). Therefore, HPL-A3 was selected and used for further experiments.

Time- and Concentration-Dependent Changes in the RIF-Mediated Induction of CALUX HPL-A3 was treated with RIF (10 μM), and the induced luciferase activities were measured at the indicated times. The luciferase activity increased in a time-dependent fashion up to 24 h after RIF-treatment and thereafter gradually decreased (Fig. 2A). Therefore, the reaction time was fixed at 24 h, and the concentration-effect of RIF on the induction of luciferase was further examined. RIF-mediated increases in luciferase activity occurred in a concentration-dependent fashion up to 100 μM (Fig. 2B).

RIF-Mediated Induction of CYP3A Subfamily Enzymes We first examined the induction of CYP3A enzyme activity according to the CYP3A4 p450-Glo™ Biochemical and Cell-Based Assay. The constitutive CYP3A activity in HPL-A3 was 0.107±0.036 RLU/μg protein, while in its parental cell line, HepG2, no CYP3A activity was detected. The time-dependent change in enzyme activity after treatment of HPL-A3 with RIF (10 μM) was then examined. The RIF-mediated increase in enzyme activity occurred in a time-dependent fashion up to 48 h, and the increased level at 48 h was maintained for up to 96 h (Fig. 3A). Considering such time-dependent induction, the concentration-effect of RIF was further assessed at 24 h. The RIF-mediated increase in CYP3A enzyme activity occurred in a concentration-dependent fashion up to 30 μM (Fig. 3B), while

Table 2. RIF-Mediated Induction of CALUX Activity in the Established Clones

Clone	Luciferase activity (luminescence unit/mg protein)		Induction ratio (RIF/CONT)
	CONT	10 μM RIF	
HPL-A3	4171±152	66958±2390**	16.05
HPL-A7	159186±1369	533185±8035**	3.35
HPL-A11	371±38	1020±45**	2.75
HPL-A12	275±17	1340±187**	4.87
HPL-A13	32895±2164	149212±7809**	4.54
HPL-A14	7844±6307	7743±3278	0.99
HPL-A17	105±2	121±5*	1.16
HPL-A18	107±11	118±5	1.10

The eight G418-resistant HepG2 clones, which stably express both PXR and luciferase, were treated with RIF or vehicle alone (CONT, 0.1% DMSO) for 24 h. Total cell lysates were prepared and used for the CALUX assay. The values represent the mean±S.E. in vehicle- and RIF-treated groups (n=3), respectively. *,** Significant differences from the corresponding vehicle-treated groups were assayed by Student's *t*-test; *$p<0.05$, **$p<0.01$.

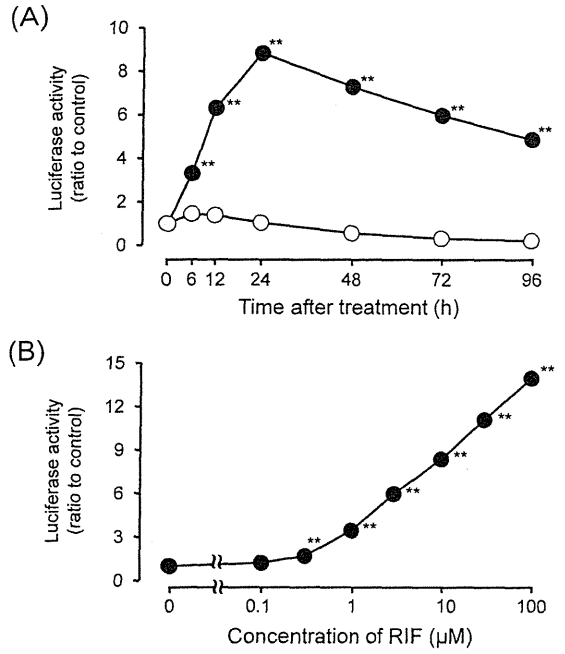

Fig. 2. Time–Course or Dose-Dependent Changes in CALUX in HPL-A3 after Treatment with RIF

HPL-A3 cells were treated with RIF (10 μM) or with vehicle alone (0.1% DMSO) for the indicated times (A) or were treated with RIF at the indicated concentrations for 24 h (B), and total cell lysates were used for the CALUX assay. The luciferase activity was measured as described in the Materials and Methods, and the data are represented as a ratio relative to corresponding controls. Solid and open circles represent the mean in RIF- and vehicle-treated groups, respectively (n=4), and the bars show their standard errors. **Significant differences from the corresponding controls assayed by ANOVA and Dunnett's test; **p<0.01.

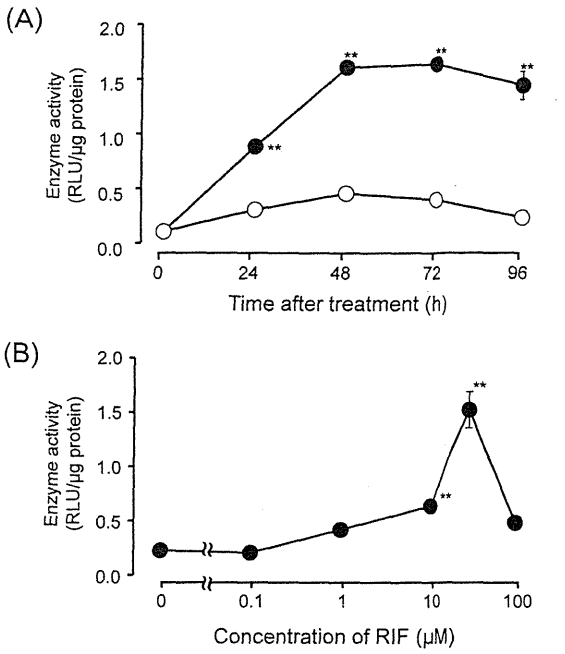

Fig. 3. Time–Course or Dose-Dependent Changes in the Activity of CYP3A Subfamily Enzymes in HPL-A3 after Treatment with RIF

HPL-A3 cells were treated with RIF (10 μM) or with vehicle alone (0.1% DMSO) for the indicated times (A) or were treated with RIF at various concentrations for 24 h (B). CYP3A enzyme activity was assessed by p450-Glo CYP3A4 assays, and the data are represented as a ratio relative to the control (treated with vehicle alone). Solid and open circles represent the mean in RIF- and vehicle-treated groups, respectively (n=3), and the bars show their standard errors. **Significant differences from the corresponding controls assayed by ANOVA and Dunnett's test; **p<0.01.

no such significant increase was observed at 100 μM.

The constitutive level of *CYP3A4* expression was measured by a real-time RT-PCR method. The constitutive *CYP3A4* expression level in HPL-A3 was 1.6-fold higher than in HepG2. Subsequently, the time-dependent change in the level of *CYP3A4* expression after treatment with RIF (10 μM) was examined. The expression level was increased in a time-dependent fashion up to 24 h (Fig. 4A). The increased level was maintained for up to 48 h and thereafter gradually decreased. *CYP3A4* expression at 24 h was about 5-fold higher than the corresponding control level. In addition, 24 h after the RIF treatment, the expression levels of *CYP3A5* and *CYP3A7* were likewise increased 3–3.5-fold compared with the corresponding control levels (data not shown). A concentration-effect of RIF on expression of *CYP3A4* was further examined at 24 h after RIF-treatment. *CYP3A4* expression was increased in a concentration-dependent fashion up to 100 μM (Fig. 4B). Moreover, there was a significantly positive correlation between the CALUX (luciferase activity) and the gene expression of CYP3A4 (Fig. 4C).

Usefulness of HPL-A3 for Screening Human CYP3A Inducers It has been reported that species specificity in the induction of CYP3A subfamily enzymes by xenobiotics is likely to be a consequence of differences at the level of PXR activation.[25,26] Therefore, we comparatively examined the effects of the human and/or rodent PXR ligands on the inductions of CALUX and CYP3A4 mRNA in HPL-A3. In this experiment, human PXR activators (RIF and CLO), human/mouse/rat PXR activators (TAM and NIC), and mouse/rat PXR activators (DEX and PCN) were used as representative species-selective PXR activators.[27–30] The working concentration of each chemical (10 μM) was determined on the basis of previously reported data.[14,28,30]

Treatments of HPL-A3 with RIF, CLO, TAM and NIC for 24 h resulted in significant increases in CALUX, represented as luciferase activity (Fig. 5A). On the other hand, no significant increases by DEX and PCN were observed. Significant increases in the level of *CYP3A4* expression was likewise observed in HPL-A3 treated with RIF, CLO, TAM or NIC, but not with DEX and PCN (Fig. 5B). Furthermore, there were significantly positive correlations between CALUX and the level of *CYP3A4* expression in the chemical-treated HPL-A3 cells (Fig. 5C).

Induction of CALUX by Calcium Channel Blockers We have previously reported that several dihydropyridine calcium channel blockers (CCBs), especially NIC, showed abilities to induce hepatic CYP3A subfamily enzymes in rats and mice.[31–33] Therefore, the effects on CALUX of CCBs, such as NIC, NIF, NIM, NIT or NIS, were assessed using HPL-A3 cells. The CALUX assay was performed 24 h after incubation with each CCB. The increases in CALUX in response to all the CCBs used occurred in a concentration-dependent fashion (Fig. 6). In addition, NIS showed cytocidal effects on HPL-A3 cells at concentrations of more than 10 μM. When the effects on the induction of CALUX were compared among CCBs at 3 μM, they were active in the following order: NIM>NIC, NIT>NIS, NIF.

Gene Expression of Positive Transcriptional Regulators

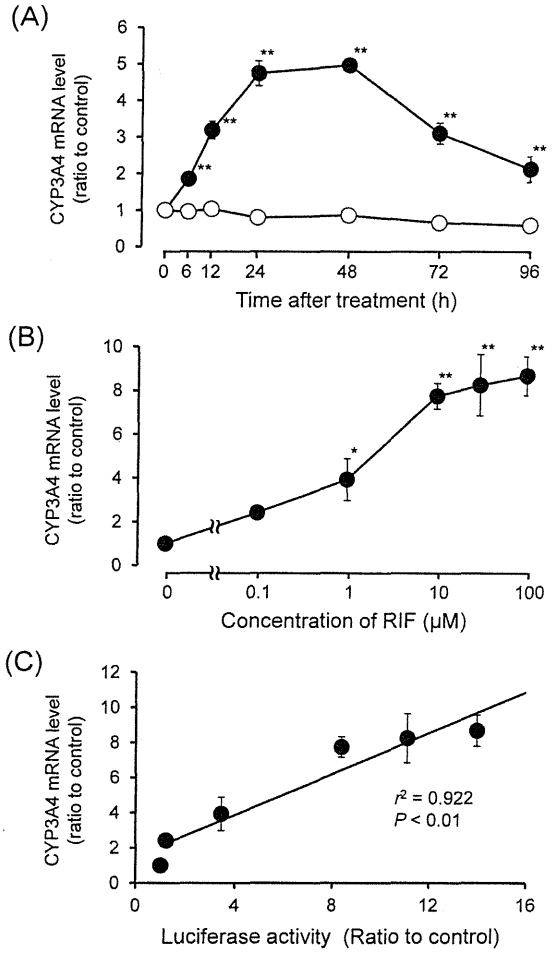

Fig. 4. Time–Course or Dose-Dependent Changes in the Level of CYP3A4 mRNA in HPL-A3 after Treatment with RIF

HPL-A3 cells were treated with RIF (10 μM) or with a vehicle alone (0.1% DMSO) for the indicated times (A) or were treated with RIF at the indicated concentrations for 24 h (B), and the total RNA from the cells was used for real-time RT-PCR analysis. The level of CYP3A4 mRNA was normalized to that of GAPDH mRNA and represented as a ratio relative to the corresponding controls. The correlations between luciferase activities (as shown in Fig. 2B) and the levels of CYP3A4 mRNA after the treatment with RIF at various concentrations for 24 h were assessed by regression analysis (C). Solid and open circles represent the means of RIF- and vehicle-treated groups (n=3), respectively, and the bars show their standard errors. ***Significant differences from the corresponding controls assayed by ANOVA and Dunnett's test; *p<0.05, **p<0.01.

of the *CYP3A4* Gene It has been reported that not only PXR but also CAR and VDR are associated with chemical-mediated activation of *CYP3A4* expression.[8,9] Therefore, we examined the constitutive gene expression levels of PXR, CAR, and VDR in HPL-A3 cells, and their levels were compared with those in HepG2. Likewise, the gene expression levels of RXRα, a partner protein for PXR, CAR, and VDR, were comparatively examined. As expected, the constitutive expression level of *PXR* in HPL-A3, which is transfected with an hPXR expression vector, was higher than in the HepG2 parental cell line (Fig. 7). On the other hand, only low level expression of *CAR* was observed in either HPL-A3 or HepG2. No clear difference in the expression level of *RXRα* between HPL-A3 and HepG2 was observed. The expression level of *VDR* was surprisingly clearly increased in HPL-A3 compared with HepG2.

VD_3-Mediated Induction of CALUX and *CYP3A4* Expression Since HPL-A3 was predicted to express VDR, the

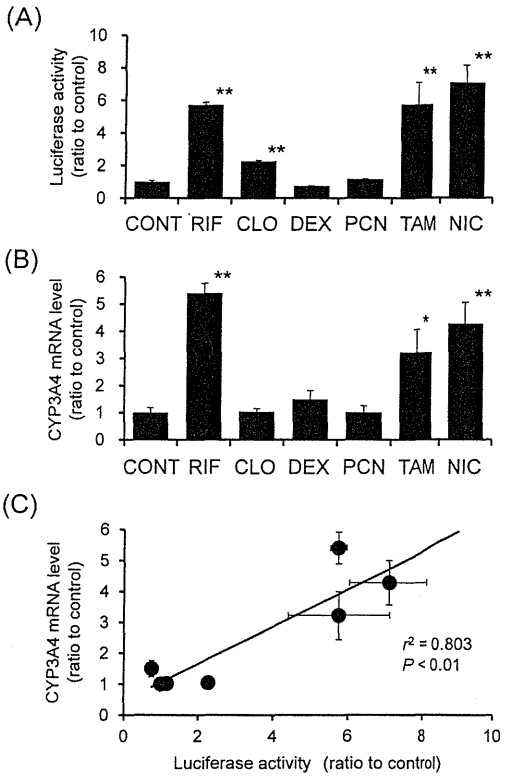

Fig. 5. Effects of Various Chemicals on the Induction of CALUX and CYP3A4 mRNA in HPL-A3

HPL-A3 cells were treated with each chemical (10 μM) for 24 h. Total cell lysates and total RNA were used for CALUX assay and real-time RT-PCR analysis, respectively. The luciferase activity is represented as a ratio relative to the control (treated with vehicle alone) (A). The level of CYP3A4 mRNA was normalized to that of GAPDH mRNA and represented as a ratio relative to the corresponding controls (B). The correlations between luciferase activities and the levels of CYP3A4 mRNA after the chemical-treatment for 24 h were assessed by regression analysis (C). ***Significant differences from the corresponding controls assayed by ANOVA and Dunnett's test; *p<0.05, **p<0.01.

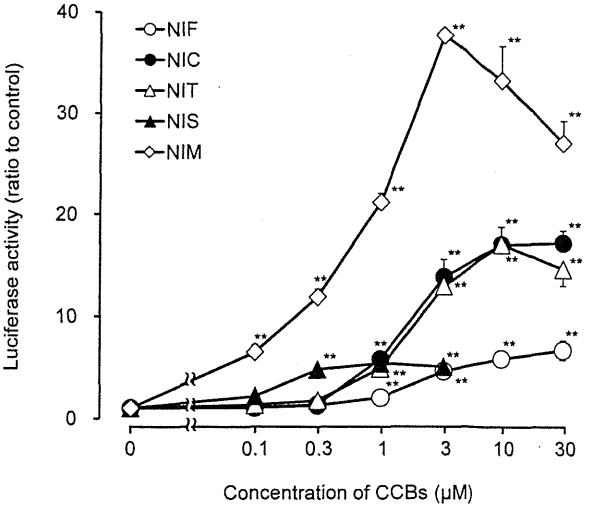

Fig. 6. Dose-Dependent Changes in CALUX in HPL-A3 Cells after Treatment with Calcium Channel Blockers

HPL-A3 cells were treated with a calcium channel blocker (NIC, NIF, NIM, NIT or NIS) at the indicated concentrations for 24 h, and total cell lysates were used for the CALUX assay. The luciferase activity is shown as a ratio relative to the control (treated with vehicle alone). The values represent the mean in each group (n=3), and the bars show their standard errors. **Significant differences from the corresponding controls assayed by ANOVA and Dunnett's test; **p<0.01.

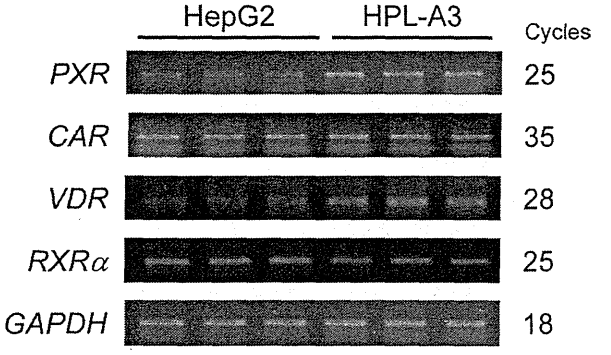

Fig. 7. Gene Expression of Positive Transcriptional Regulators of the *CYP3A4* Gene in HPL-A3 Cells and the Parental Cell Line, HepG2

Total RNA was prepared from HPL-A3 or HepG2 cells and used for conventional RT-PCR analyses of PXR, VDR, CAR and RXRα mRNAs. *GAPDH* was used as an internal standard. The PCR products were separated by electrophoresis on a 2% agarose gel and visualized by ethidium bromide staining under UV light.

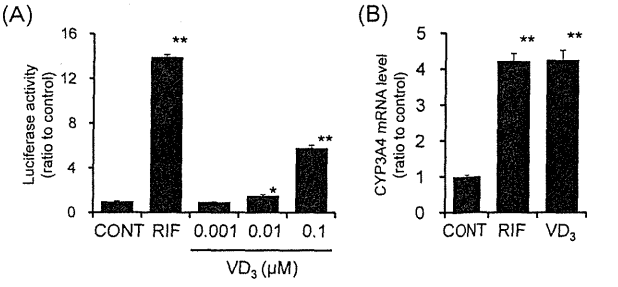

Fig. 8. Effects of VD_3 on the Induction of CALUX and CYP3A4 mRNA in HPL-A3

HPL-A3 cells were treated with VD_3 at the indicated concentrations for 24 h, and their total cell lysates were used for the CALUX assay. RIF (10 μM) was used as a positive control. The luciferase activity is represented as a ratio relative to the control (treated with vehicle alone) (A). The real-time RT-PCR analysis for CYP3A4 mRNA was performed using cells treated with VD_3 (0.1 μM) or RIF (10 μM) for 24 h (B). The level of CYP3A4 mRNA was normalized to that of GAPDH mRNA and represented as a ratio relative to the corresponding controls. The solid columns represent the mean in each group (n=3), and the bars show their standard errors. *** Significant differences from the corresponding controls assayed by ANOVA and Dunnett's test; $*p<0.05$, $**p<0.01$.

effects of VD_3, a VDR ligand, on the induction of CALUX and CYP3A4 mRNA were examined. The working concentration (0.1 μM) of VD_3 was determined on the basis of previously reported data.[8,34]

After VD_3-treatment, luciferase activity was increased in a time-dependent fashion up to 24 h (data not shown). Therefore, the reaction time was fixed at 24 h, and the concentration-effect of VD_3 on the induction of CALUX was examined. CALUX induction occurred in a concentration-dependent fashion in the range of 0.01–0.1 μM (Fig. 8A). In addition, a significant increase in *CYP3A4* expression was confirmed in HPL-A3 treated with VD_3 (0.1 μM) for 24 h (Fig. 8B).

DISCUSSION

In the present study, we established an HPL-A3 cell line by co-transfection of the p3A4-hPXRE-Luc reporter plasmid and an hPXR expression plasmid into HepG2 cells, and the applicability of the cell line to the hPXR-based CALUX assay was first assessed using RIF, a representative hPXR activator. The time- and concentration-dependent inductions of CALUX and *CYP3A4* expression by RIF were clearly observed in HPL-A3, and significantly positive correlation between CALUX (luciferase activity) and *CYP3A4* expression was also observed. In addition, RIF-mediated induction of CYP3A enzyme activity occurred in a concentration-dependent fashion up to 30 μM, but at a higher concentration (100 μM), the increased activity was reduced. These phenomena can be attributed to the biochemical properties of RIF; it has the ability not only to induce CYP3A subfamily enzymes[35] but also to inhibit the activities of several CYP enzymes, including CYP3A4.[36]

CALUX in HPL-A3 was further increased not only by hPXR-selective activators (RIF and CLO) but also by human/mouse/rat PXR activators (TAM and NIC), while no such significant increases by mouse/rat PXR activators (DEX and PCN) were observed. These results suggest that HPL-A3 is adaptable for use in hPXR-based reporter gene assays.

We have previously reported that CCBs, such as NIC, NIF, NIM, NIT and NIS, show abilities to induce hepatic CYP3A subfamily enzymes in rats.[37] These CCBs are also known to have affinity to hPXR and to show the ability to activate hPXR-based reporter genes.[27,38–40] Therefore, we examined the capacities of NIC, NIF, NIM, NIT and NIS for hPXR activation using HPL-A3, and confirmed that all the CCBs used act as hPXR activators. Furthermore, we demonstrated that they were active in the following order: NIM>NIC, NIT>NIS, NIF. This order was similar to that in a previous report on the induction of hepatic *CYP3A1* in rats.[37]

To further understand the mechanisms for the xenobiotic-mediated induction of CALUX and *CYP3A4* expression in HPL-A3, we examined the gene expression of transcriptional factors, such as PXR, CAR, VDR and their partner protein (RXRα), that are involved in the regulation of *CYP3A4* expression. As expected, the expression level of *PXR* was significantly increased in HPL-A3, which is transfected with an hPXR expression vector, compared with that in the HepG2 parental cell line. The gene expression level of VDR was likewise increased. However, the mechanism for the increase in gene expression of VDR remains unclear, although the increase might be dependent on the insertion sites of the hPXR expression vector and/or the reporter plasmid p3A4-PXRE-Luc in the genome of host cells. In addition, no clear changes in the expression levels of *CAR* or *RXRα* by the insertion of the expression vector and reporter plasmid were observed in HPL-A3.

Because a high level of *VDR* expression is predicted in HPL-A3, we further examined whether VD_3, a representative ligand of hVDR, can induce CALUX and CYP3A4 mRNA in HPL-A3 cells, and we indeed demonstrated VD_3-mediated inductions. Although the expression level of VDR is not especially high in human hepatocytes,[41,42] it has been reported that the activation of VDR led to modifications in the expression of hepatic CYPs, such as CYP3A4,[8] CYP7A1 and CYP24A1,[10] and to altered hepatic lipid metabolism.[43] The previous and present findings therefore suggest that HPL-A3 is a useful tool for the screening of hVDR activators/inhibitors and for the analysis of hVDR function in the liver.

In conclusion, we have established an HPL-A3 cell line, which is a useful tool for the screening of not only human CYP3A inducers but also the activators/inhibitors of CYP3A transcription factors, such as hPXR and hVDR. Studies on the altered expression of CYP3A subfamily enzymes, especially

CYP3A4, by xenobiotics such as drugs are important for understanding the therapeutic/toxic effects of drugs and environmental chemicals. Therefore, the established HPL-A3 cell line will greatly contribute to the development of these studies.

Acknowledgments We thank Ms. K. Yabe and Mr. S. Hirai (Department of Molecular Toxicology, School of Pharmaceutical Sciences, University of Shizuoka) for assistance with experiments in this study. This work was supported in part by a Research Grant-in-Aid from the Ministry of Health, Labour and Welfare of Japan (M.D.).

REFERENCES

1) Danielson PB. The cytochrome P450 superfamily: biochemistry, evolution and drug metabolism in humans. *Curr. Drug Metab.*, **3**, 561–597 (2002).
2) Zhou SF. Drugs behave as substrates, inhibitors and inducers of human cytochrome P450 3A4. *Curr. Drug Metab.*, **9**, 310–322 (2008).
3) Tachibana T, Kato M, Takano J, Sugiyama Y. Predicting drug–drug interactions involving the inhibition of intestinal CYP3A4 and P-glycoprotein. *Curr. Drug Metab.*, **11**, 762–777 (2010).
4) Donato MT, Lahoz A, Castell JV, Gómez-Lechón MJ. Cell lines: a tool for *in vitro* drug metabolism studies. *Curr. Drug Metab.*, **9**, 1–11 (2008).
5) Aninat C, Piton A, Glaise D, Le Charpentier T, Langouët S, Morel F, Guguen-Guillouzo C, Guillouzo A. Expression of cytochromes P450, conjugating enzymes and nuclear receptors in human hepatoma HepaRG cells. *Drug Metab. Dispos.*, **34**, 75–83 (2006).
6) Kliewer SA, Moore JT, Wade L, Staudinger JL, Watson MA, Jones SA, McKee DD, Oliver BB, Willson TM, Zetterström RH, Perlmann T, Lehmann JM. An orphan nuclear receptor activated by pregnanes defines a novel steroid signaling pathway. *Cell*, **92**, 73–82 (1998).
7) Lehmann JM, McKee DD, Watson MA, Willson TM, Moore JT, Kliewer SA. The human orphan nuclear receptor PXR is activated by compounds that regulate CYP3A4 gene expression and cause drug interactions. *J. Clin. Invest.*, **102**, 1016–1023 (1998).
8) Drocourt L, Ourlin JC, Pascussi JM, Maurel P, Vilarem MJ. Expression of CYP3A4, CYP2B6, and CYP2C9 is regulated by the vitamin D receptor pathway in primary human hepatocytes. *J. Biol. Chem.*, **277**, 25125–25132 (2002).
9) Moore LB, Parks DJ, Jones SA, Bledsoe RK, Consler TG, Stimmel JB, Goodwin B, Liddle C, Blanchard SG, Willson TM, Collins JL, Kliewer SA. Orphan nuclear receptors constitutive androstane receptor and pregnane X receptor share xenobiotic and steroid ligands. *J. Biol. Chem.*, **275**, 15122–15127 (2000).
10) Han S, Chiang JYL. Mechanism of vitamin D receptor inhibition of cholesterol 7α-hydroxylase gene transcription in human hepatocytes. *Drug Metab. Dispos.*, **37**, 469–478 (2009).
11) Raucy J, Warfe L, Yueh MF, Allen SW. A cell-based reporter gene assay for determining induction of CYP3A4 in a high-volume system. *J. Pharmacol. Exp. Ther.*, **303**, 412–423 (2002).
12) Lemaire G, de Sousa G, Rahmani R. A PXR reporter gene assay in a stable cell culture system: CYP3A4 and CYP2B6 induction by pesticides. *Biochem. Pharmacol.*, **68**, 2347–2358 (2004).
13) Yueh MF, Kawahara M, Raucy J. High volume bioassays to assess CYP3A4-mediated drug interactions: induction and inhibition in a single cell line. *Drug Metab. Dispos.*, **33**, 38–48 (2005).
14) Lemaire G, Mnif W, Pascussi JM, Pillon A, Rabenoelina F, Fenet H, Gomez E, Casellas C, Nicolas JC, Cavaillès V, Duchesne MJ, Balaguer P. Identification of new human pregnane X receptor ligands among pesticides using a stable reporter cell system. *Toxicol. Sci.*, **91**, 501–509 (2006).
15) Noracharttiyapot W, Nagai Y, Matsubara T, Miyata M, Shimada M, Nagata K, Yamazoe Y. Construction of several human-derived stable cell lines displaying distinct profiles of CYP3A4 induction. *Drug Metab. Pharmacokinet.*, **21**, 99–108 (2006).
16) Goodwin B, Hodgson E, Liddle C. The orphan human pregnane X receptor mediates the transcriptional activation of CYP3A4 by rifampicin through a distal enhancer module. *Mol. Pharmacol.*, **56**, 1329–1339 (1999).
17) Sekimoto M, Iwamoto M, Miyajima S, Nemoto K, Degawa M. Establishment of a rat hepatic cell line, KanR2-XL8, for a reporter gene assay of aryl hydrocarbon receptor ligands. *J. Health Sci.*, **50**, 530–536 (2004).
18) Sekimoto M, Kawamagari H, Nakatani S, Nemoto K, Degawa M. Establishment of a human hepatoma cell line HepG2-A10 for a reporter gene assay of arylhydrocarbon receptor activators. *Genes Environ.*, **29**, 11–16 (2007).
19) Dotzlaw H, Leygue E, Watson P, Murphy LC. The human orphan receptor PXR messenger RNA is expressed in both normal and neoplastic breast tissue. *Clin. Cancer Res.*, **5**, 2103–2107 (1999).
20) Malaplate-Armand C, Ferrari L, Masson C, Visvikis-Siest S, Lambert H, Batt AM. Down-regulation of astroglial CYP2C, glucocorticoid receptor and constitutive androstane receptor genes in response to cocaine in human U373 MG astrocytoma cells. *Toxicol. Lett.*, **159**, 203–211 (2005).
21) Matsubara T, Yoshinari K, Aoyama K, Sugawara M, Sekiya Y, Nagata K, Yamazoe Y. Role of vitamin D receptor in the lithocholic acid-mediated CYP3A induction *in vitro* and *in vivo*. *Drug Metab. Dispos.*, **36**, 2058–2063 (2008).
22) Tian W, Osawa M, Horiuchi H, Tomita Y. Expression of the prolactin-inducible protein (PIP/GCDFP15) gene in benign epithelium and adenocarcinoma of the prostate. *Cancer Sci.*, **95**, 491–495 (2004).
23) Zhuo X, Zheng N, Felix CA, Blair IA. Kinetics and regulation of cytochrome P450-mediated etoposide metabolism. *Drug Metab. Dispos.*, **32**, 993–1000 (2004).
24) Cali JJ, Ma D, Sobol M, Simpson DJ, Frackman S, Good TD, Daily WJ, Liu D. Luminogenic cytochrome P450 assays. *Expert Opin. Drug Metab. Toxicol.*, **2**, 629–645 (2006).
25) Jones SA, Moore LB, Shenk JL, Wisely GB, Hamilton GA, McKee DD, Tomkinson NC, LeCluyse EL, Lambert MH, Willson TM, Kliewer SA, Moore JT. The pregnane X receptor: a promiscuous xenobiotic receptor that has diverged during evolution. *Mol. Endocrinol.*, **14**, 27–39 (2000).
26) LeCluyse EL. Pregnane X receptor: molecular basis for species differences in CYP3A induction by xenobiotics. *Chem. Biol. Interact.*, **134**, 283–289 (2001).
27) Drocourt L, Pascussi JM, Assenat E, Fabre JM, Maurel P, Vilarem MJ. Calcium channel modulators of the dihydropyridine family are human pregnane X receptor activators and inducers of CYP3A, CYP2B, and CYP2C in human hepatocytes. *Drug Metab. Dispos.*, **29**, 1325–1331 (2001).
28) Vignati LA, Bogni A, Grossi P, Monshouwer M. A human and mouse pregnane X receptor reporter gene assay in combination with cytotoxicity measurements as a tool to evaluate species-specific CYP3A induction. *Toxicology*, **199**, 23–33 (2004).
29) Sane RS, Buckley DJ, Buckley AR, Nallani SC, Desai PB. Role of human pregnane X receptor in tamoxifen- and 4-hydroxytamoxifen-mediated CYP3A4 induction in primary human hepatocytes and LS174T cells. *Drug Metab. Dispos.*, **36**, 946–954 (2008).
30) Cui X, Thomas A, Gerlach V, White RE, Morrison RA, Cheng KC. Application and interpretation of hPXR screening data: Validation of reporter signal requirements for prediction of clinically relevant CYP3A4 inducers. *Biochem. Pharmacol.*, **76**, 680–689 (2008).
31) Konno Y, Nemoto K, Degawa M. Induction of hepatic cytochrome P450s responsible for the metabolism of xenobiotics by nicardipine and other calcium channel antagonists in the male rat. *Xenobiotica*, **33**, 119–129 (2003).
32) Konno Y, Sekimoto M, Nemoto K, Degawa M. Sex difference in

induction of hepatic CYP2B and CYP3A subfamily enzymes by nicardipine and nifedipine in rats. *Toxicol. Appl. Pharmacol.*, **196**, 20–28 (2004).
33) Konno Y, Sekimoto M, Nemoto K, Degawa M. Induction of hepatic Cyp2b and Cyp3a subfamily enzymes by nicardipine and nifedipine in mice. *Xenobiotica*, **34**, 607–618 (2004).
34) Khan AA, Chow ECY, van Loenen-Weemaes AMMA, Porte RJ, Pang KS, Groothuis GMM. Comparison of effects of VDR *versus* PXR, FXR and GR ligands on the regulation of CYP3A isozymes in rat and human intestine and liver. *Eur. J. Pharm. Sci.*, **37**, 115–125 (2009).
35) Gillum JG, Israel DS, Polk RE. Pharmacokinetic drug interactions with antimicrobial agents. *Clin. Pharmacokinet.*, **25**, 450–482 (1993).
36) Kajosaari LI, Laitila J, Neuvonen PJ, Backman JT. Metabolism of repaglinide by CYP2C8 and CYP3A4 *in vitro*: effect of fibrates and rifampicin. *Basic Clin. Pharmacol. Toxicol.*, **97**, 249–256 (2005).
37) Konno Y, Degawa M. Gene activations of CYP2B1 and CYP3A1 by dihydropyridine calcium channel antagonists in the rat liver: the structure–activity relationship. *Biol. Pharm. Bull.*, **27**, 903–905 (2004).
38) Pan Y, Li L, Kim G, Ekins S, Wang H, Swaan PW. Identification and validation of novel human pregnane X receptor activators among prescribed drugs *via* ligand-based virtual screening. *Drug Metab. Dispos.*, **39**, 337–344 (2011).
39) Shukla SJ, Sakamuru S, Huang R, Moeller TA, Shinn P, Vanleer D, Auld DS, Austin CP, Xia M. Identification of clinically used drugs that activate pregnane X receptors. *Drug Metab. Dispos.*, **39**, 151–159 (2011).
40) Xiao L, Nickbarg E, Wang W, Thomas A, Ziebell M, Prosise WW, Lesburg CA, Taremi SS, Gerlach VL, Le HV, Cheng KC. Evaluation of *in vitro* PXR-based assays and *in silico* modeling approaches for understanding the binding of a structurally diverse set of drugs to PXR. *Biochem. Pharmacol.*, **81**, 669–679 (2011).
41) Nishimura M, Naito S, Yokoi T. Tissue-specific mRNA expression profiles of human nuclear receptor subfamilies. *Drug Metab. Pharmacokinet.*, **19**, 135–149 (2004).
42) Bookout AL, Jeong Y, Downes M, Yu RT, Evans RM, Mangelsdorf DJ. Anatomical profiling of nuclear receptor expression reveals a hierarchical transcriptional network. *Cell*, **126**, 789–799 (2006).
43) Wang JH, Keisala T, Solakivi T, Minasyan A, Kalueff AV, Tuohimaa P. Serum cholesterol and expression of ApoAI, LXRβ and SREBP2 in vitamin D receptor knock-out mice. *J. Steroid Biochem. Mol. Biol.*, **113**, 222–226 (2009).

Toxicology in Vitro 25 (2011) 1320–1327

Contents lists available at ScienceDirect

Toxicology in Vitro

journal homepage: www.elsevier.com/locate/toxinvit

Effect of interaction between phenolic compounds and copper ion on antioxidant and pro-oxidant activities

Yusuke Iwasaki [a], Takayuki Hirasawa [a], Yosuke Maruyama [a], Yuji Ishii [b], Rie Ito [a], Koichi Saito [a], Takashi Umemura [b], Akiyoshi Nishikawa [b], Hiroyuki Nakazawa [a,*]

[a] Department of Analytical Chemistry, Faculty of Pharmaceutical Sciences, Hoshi University, 2-4-41 Ebara, Shinagawa-ku, Tokyo 142-8501, Japan
[b] Division of Pathology, National Institute of Health Sciences, 1-18-1 Kamiyoga, Setagaya-ku, Tokyo 158-8501, Japan

ARTICLE INFO

Article history:
Received 1 December 2010
Accepted 26 April 2011
Available online 10 May 2011

Keywords:
Antioxidant
Pro-oxidant
Phenolic compound
Electron spin resonance
DNA damage

ABSTRACT

Phenolic compounds are widely used in food and cosmetics to prevent undesirable oxidation. On the other hand, phenolic compounds are also strong reducing agents and under *in vitro* conditions and in the presence of copper ion, they can act as pro-oxidants. In this study, we conducted electron spin resonance (ESR) measurements for the increase in reactive oxygen species (ROS) in relation to their structure and interaction with transition metals. Moreover, the antioxidant activity was assessed with the 1,1-diphenyl-2-picrylhydrazyl (DPPH) assay, and the pro-oxidant effect of phenolic compounds on DNA damage was assessed by measuring 8-hydroxy-2′-deoxyguanosine (8-OHdG), which is effectively formed during oxidative damage. In conclusion, *ortho*-dihydroxyl groups that can chelate with Cu^{2+} induce the greatest pro-oxidant activity. Moreover, the interaction between phenolic compounds and copper induced to H_2O_2. The obtained results indicated that ROS participated in oxidative DNA damage induced by phenolic compounds in the presence of Cu^{2+}.

1. Introduction

Phenolic compounds are widely studied for their antioxidant properties. The notion of cancer chemoprevention through intervention with an antioxidant arises from the fact that fruits and vegetables contain antioxidants that are said to lower the risk of cancer in people who consume them. In contrast, a recent meta-analysis of the clinical data from 68 randomized human trials involving 232,606 subjects (385 publications) revealed that an increased risk of mortality was associated with the regular use of certain putative antioxidant supplements, such as vitamins A and E (Bjelakovic et al., 2007). They concluded that antioxidant supplements seem to increase the risk of mortality. Those studies indicate the need to assess phenolic compounds because those compounds have antioxidant activity. Antioxidant activity refers to the ability of phenolic compounds to prevent damage caused by reactive oxygen species (ROS) (such as through radical scavenging) or to prevent the generation of ROS (by binding iron) (Perron and Brumaghim, 2009). Phenolic compounds are divided into several sub-classes, including catechins, flavonols, flavones, anthocyanins, proanthocyanidins, and phenolic acids. Phenolic compounds are present in milligram quantities in one serving of green tea (Cabrera et al., 2006), black tea (Gardner et al., 2007), coffee (Nardini et al., 2002), fruits (Vinson et al., 2001), vegetables (Vinson et al., 1998), olive oil (Del Carlo et al., 2004), or red and white wine (Lodovici et al., 2001; Makris et al., 2003). The US government has acknowledged that people whose diets are rich in fruits and vegetables may consume one gram or more per day of polyphenol compounds, based on the recommendation of 5 servings/day of colored fruits and vegetables. Because it is believed that a diet rich in fruits and vegetables is consistently associated with a decreased risk of cancer, it is highly desirable to understand the biological function and mode of activity of polyphenols (Yao et al., 2004).

Copper and iron are major metal ions present in serum (Kanabrocki et al., 2008) and tissue (Al-Ebraheem et al., 2009). Furthermore, copper is an important metal ion present in chromatin and is closely associated with DNA bases, particularly guanine (Kagawa et al., 1991). Copper supplementation is believed to be a potential therapeutic tool for the treatment and prevention of involutional osteoporosis (Rico et al., 2000). Phenolic compounds are reducing agents and under *in vitro* conditions and in the presence of metal ions, such as copper or iron, they can act as pro-oxidants (Cao et al., 1997; Sugihara et al., 1999). Phenolic anti-

Abbreviations: ESR, electron spin resonance; ROS, reactive oxygen species; 8-OHdG, 8-hydroxy-2′-deoxyguanosine; CaA, caffeic acid; ChA, chlorogenic acid; FA, ferulic acid; QA, quinic acid; Que, quercetin; Res, resveratrol; C, catechin; CG, catechin gallate; EC, epicatechin; ECG, epicatechin gallate; GC, gallocatechin; GCG, gallocatechin gallate; EGC, epigallocatechin; EGCG, epigallocatechin gallate.

* Corresponding author. Tel./fax: +81 3 5498 5765.
E-mail address: nakazawa@hoshi.ac.jp (H. Nakazawa).

0887-2333/$ - see front matter © 2011 Elsevier Ltd. All rights reserved.
doi:10.1016/j.tiv.2011.04.024

oxidants, including quercetin (Yamashita et al., 1999), curcumin (Ahsan and Hadi, 1998), tea catechins (Hayakawa et al., 1997), salsolinol (Jung and Surh, 2001), and resveratrol (Ahmad et al., 2005), were reported to induce lipid peroxidation and/or DNA damage in the presence of cupric ions. In this reaction, Cu^{2+} is reduced to Cu^{+} by phenolic compounds and the re-oxidation of Cu^{+} to Cu^{2+} is accompanied by the formation of ROS. Therefore, it is interesting to see how an antioxidant can switch to a pro-oxidant and its biological implications.

Recent studies have demonstrated that the pro-oxidant action of various phenolic compounds is attributed to the accelerated lipid peroxidation and/or induction of DNA damage, mutagenesis, carcinogenesis, and apoptosis in cancer cells (Zheng et al., 2006; Zheng et al., 2008; Wang et al., 2008). The initial electron-transfer oxidation of phenolic compounds, particularly hydroxycinnamic acid, by Cu^{2+} generates the corresponding semiquinone radical and the radical undergoes a second electron-transfer reaction with O_2 to form *ortho*-quinone and superoxide anion ($O_2^{\cdot-}$). $O_2^{\cdot-}$ reacts with Cu^{+} to give hydrogen peroxide (H_2O_2), which is readily converted via a Fenton-type reaction into hydroxyl radical (·OH) (Fan et al., 2009). ROS, such as .OH and $O_2^{\cdot-}$, is generated by these mechanisms.

In this study, we conducted electron spin resonance (ESR) measurements for the increase in ROS in relation to its structure and interaction with transition metals. Moreover, the antioxidant activity was assessed with the 1,1-diphenyl-2-picrylhydrazyl (DPPH) assay, and the pro-oxidant effect of phenolic compounds on DNA damage was assessed by measuring 8-hydroxy-2′-deoxyguanosine (8-OHdG), which is effectively formed during oxidative damage.

2. Materials and methods

2.1. Reagents and chemicals

Caffeic acid (CaA), *trans*-4-hydroxy-3-methoxycinnamic acid (Ferulic acid, FA), quercetin dihydrate (Que), rutin, (−)-epigallocatechin (EGC), (−)-epicatechin (EC), and gallocatechin (GC) were obtained from Wako Pure Chemical Industries (Tokyo, Japan). Chlorogenic acid hydrate (ChA), D-(−)-quinic acid (QA), resveratrol (Res), and (+)-catechin (C) were provided by Tokyo Chemical Industry (Tokyo, Japan). (−)-Epigallocatechin gallate (EGCG), (−)-epicatechin gallate (ECG), (−)-gallocatechin gallate (GCG), and (−)-catechin gallate (CG) were purchased from Sigma (Tokyo, Japan).

5,5′-Dimethyl-1-pyrroline-*N*-oxide (DMPO) and α-(4-pyridyl-1-oxide)-*N*-*tert*-butylnitrone (POBN) were purchased from Labotech Co. (Tokyo, Japan). Dimethyl sulfoxide (DMSO), hydrogen peroxide (30%), and 1,1-diphenyl-2-picrylhydrazyl (DPPH) were obtained from Wako Pure Chemical Industries (Tokyo, Japan). Copper(II) sulfate pentahydrate was purchased from Kanto Chemical (Tokyo, Japan). Ethylenediamine-*N*,*N*,*N*′,*N*′-tetraacetic acid, disodium salt (EDTA), and bathocuproinedisulfonic acid, disodium salt were obtained from Dojindo Laboratories (Kumamoto, Japan). Catalase and superoxide dismutase (SOD) were purchased from Sigma (Tokyo, Japan).

Deoxyribonucleic acid sodium salt from calf thymus, phosphatase alkaline from bovine intestinal mucosa, deoxyguanosine (dG), and 8-hydroxy-2′-deoxyguanosine (8-OHdG) were obtained from Sigma (Tokyo, Japan). Nuclease P1 and a DNA extractor kit were purchased from Wako Pure Chemical Industries (Tokyo, Japan).

2.2. DPPH radical-scavenging activity

The modified DPPH method was used for the determination of antioxidant activity (Szydłowska-Czerniak et al., 2010). DPPH radical solution (2 mM) was prepared in methanol and the phenolic compounds were diluted in methanol to 0.02, 0.1, 0.2, and 0.4 mM. In a 1.5 mL disposable tube, the prepared DPPH (250 μL) solution was added to a sample of diluted phenolic compound (250 μL). After 37 °C for 30 min incubation, the absorbance was read at 540 nm and scavenging activity was determined with the following equation: % scavenging activity = $[A_{control} - A_{sample}]$ $A_{control} \times 100$. The data presented are means ± SD of three determinations.

2.3. Electron spin resonance measurement of hydroxyl radical

The analysis of ·OH was carried out with an ESR spectrometer (JES-RE1X, JEOL Co., Tokyo, Japan). The ESR spectrum was measured at a microwave frequency of 9.43 GHz, a magnetic field of 335.5 ± 5 mT, a microwave power of 9 mW, a modulation of 100 kHz, a time constant of 0.03 s, and a sweep time of 30 s, using the ESR spectrometer. The spectra of the samples were scanned to record the signal intensities (peak-to-peak heights).

A typical incubation consisted of phosphate buffer (50 mM, pH 7.4), POBN (10 mM), DMSO (10%), phenolic compounds (2 mM), and copper(II) sulfate pentahydrate (1 mM) in a final volume of 0.3 mL. Samples were taken at a reaction at 37 °C for 30 min.

2.4. DNA digestion and determination of dG and 8-OHdG

In order to prevent the formation of oxidative by-products during DNA isolation, DNA was digested by using the slightly modified method (Ishii et al., 2007). Calf thymus DNA (2 mg/mL) 250 μL was incubated at 37 °C for 30 min after adding 50 μL of phenolic compounds (2 mM) and 50 μL of copper(II) sulfate pentahydrate (1 mM) in 0.15 mL of phosphate buffer (50 mM, pH 7.4). Treated calf thymus DNA was immediately centrifuged at 10,000g for 5 min at 10 °C after the total volume was adjusted to 1.5 mL by adding NaI and 2-propanol. After washing with ethanol, the pellet was dissolved in 0.2 mL of 20 mM sodium acetate buffer, pH 4.8. DNA was enzymatically hydrolyzed by adding 5.0 μL of nuclease P1 to obtain a concentration of 500 units/mL. The mixture was incubated at 60 °C for 15 min. After the addition of 20 μL of 1.0 M Tris–HCl buffer (pH 8.0), 5.0 μL of alkaline phosphatase was added to give a final concentration of 20 units/mL. The mixture was passed through a 3000 NMWL filter (Millipore, Tokyo, Japan) after incubating at 37 °C for 60 min. Then, the digested solution was injected into the LC-UV-ECD instrument for 8-OHdG and dG analysis.

2.5. HPLC-UV-ECD conditions for dG and 8-OHdG analysis

In the dG and 8-OHdG assay, the UV detector and the ECD used were a Shimadzu SPD10A (Tokyo, Japan) and an ESA Coulochem III (Tokyo, Japan), respectively. A Shimadzu 10Avp pump (Tokyo, Japan) was used to induce flow through the analytical column. An Inertsil ODS3 (4.6 mm × 150 mm, 3.0 μm, GL Sciences, Tokyo, Japan) was used for separation. An aliquot (20 μL) of the sample was injected into the ODS column whose temperature was maintained at 40 °C. The mobile phase was a mixture of 10 mM sodium phosphate/methanol (97/3, v/v). The compounds were eluted isocratically at a flow rate of 1.0 mL/min. The wavelength of the UV detector was set at 290 nm for the detection of dG. The Coulochem III ECD was used with a guard cell (Model 5020; -350 mV), and an analytical cell (Model 5011; electrode 1, 150 mV; electrode 2, 300 mV).

2.6. Statistical analysis

All results are expressed as mean ± SD. Statistics were analyzed using one-way analysis of variance (ANOVA), and if statistically significant, *post hoc* analysis using the Dunnett method was fol-

lowed as a multiple comparison among groups. Values of $P < 0.05$ and 0.01 were considered statistically significant.

3. Results

3.1. Radical scavenging activity of phenolic compounds

The antioxidant activities of the phenolic compounds were measured by the DPPH method, which is one of the oldest and the most frequently used methods for evaluating antioxidant activity. The scavenging effects of phenolic compounds on DPPH radicals are shown in Fig. 1. All the phenolic compounds excepted QA exhibited antioxidant activities. In catechin and its related compounds, the chemical structure was a main contributor to the antioxidant activity. The DPPH radical scavenging activities of gallate groups, such as CG, ECG, GCG, and EGCG, were stronger than those of non-gallate groups. The pyrogallol group (benzene-1,2,3-triol) has stronger DPPH radical scavenging activity than the catechol group (1,2-dihydroxybenzene). Finally, epicatechin precursors, such as EC, ECG, EGC, and EGCG, exhibited antioxidant activities that were similar to or greater than those of epicatechin epimers, namely C, CG, GC, and GCG.

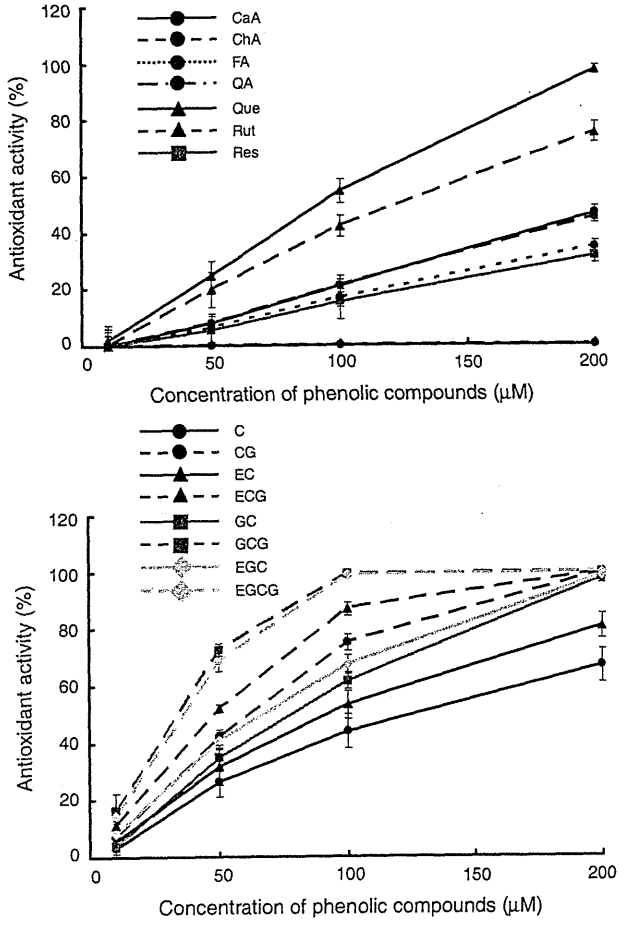

Fig. 1. Antioxidant activities of phenolic compounds as assessed by DPPH assay. DPPH concentration was 1 mM. Data points represent means ± SD ($n = 3$). CaA, caffeic acid; ChA, chlorogenic acid; FA, ferulic acid; QA, quinic acid; Que, quercetin; Res, resveratrol; C, catechin; CG, catechin gallate; EC, epicatechin; ECG, epicatechin gallate; GC, gallocatechin; GCG, gallocatechin gallate; EGC, epigallocatechin; EGCG, epigallocatechin gallate.

3.2. Assessment of POBN as spin trapping reagent

·OH is one of the most aggressive ROS. It can be generated by the interaction of metal ion and H_2O_2 (Fenton reaction) and/or $O_2^{\cdot-}$ with H_2O_2 (Haber Weiss reaction), especially in the presence of catalytic metal ions. It is important to measure such ROS as ·OH because ROS induces DNA damage, mutagenesis, and carcinogenesis. However, it is difficult to detect ·OH because of its extremely short lifetime. The most direct means to demonstrate the formation of ·OH is to quantify its radical products by ESR measurement, using either fast flow systems or spin traps that combine with reactive radicals to form more stable adducts. DMPO is used widely as a spin trapping reagent. The Fenton reaction can generate ·OH, which can be trapped by DMPO and give a typical four line ESR spectrum with intensity 1:2:2:1 ($\alpha^N = \alpha^H = 1.49$ mT). ·CH_3, which adduct of DMPO generates ESR spectrum with hyperfine splitting constants of $\alpha^N = 1.64$ mT, $\alpha^H = 2.35$ mT (Barr et al., 1996) was generated by the interaction of DMSO and ·OH (Fig. 2). When copper ion is coexistent to DMPO, DMPO–OH signal appears. If ·OH has been generated, ·CH_3 could be generated by the interaction of DMSO and ·OH. However, there is no DMPO–CH_3 signal (Fig. 3). A number of studies have suspected artificial reactions, because DMPO is affected by copper ion, and susceptible to decomposition by light and oxygen.

The most common spin trap used to trap ·CH_3 that is produced in the *in vitro* or *in vivo* reaction of DMSO with ·OH is the nitrone compound POBN. ·OH is added to DMSO and the resulting alkoxyl radicals decompose to ·CH_3, which is efficiently scavenged by POBN. The rate constant between DMSO and ·OH has been utilized to increase ESR spin trapping detection of ·OH ($k = 7 \times 10^9\ M^{-1}\ s^{-1}$) (Babbs and Steiner, 1990). The ·CH_3 adduct of POBN generates a six line ESR spectrum with hyperfine splitting constants of $\alpha^N = 1.57$ mT, $\alpha^H = 0.28$ mT (Yue Qian et al., 2005). Fig. 4 shows the ESR spectra and correlation of DMPO–OH with POBN-CH_3 using

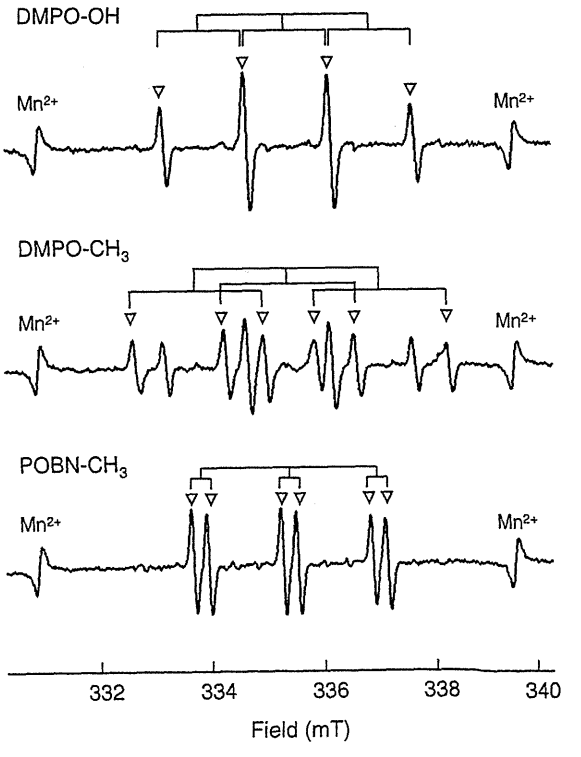

Fig. 2. ESR spectra of DMPO–OH, DMPO–CH_3, and POBN-CH_3.

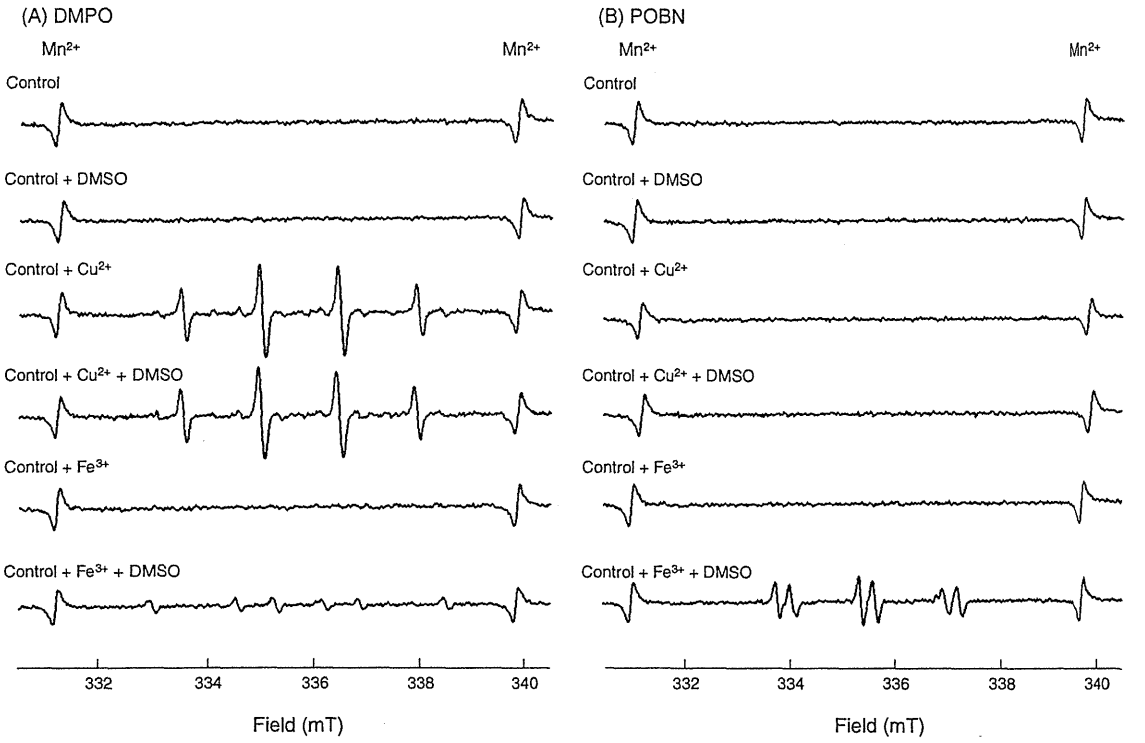

Fig. 3. ESR spectra from the reaction of spin trapping reagent with DMSO in the presence of a metal ion. (A) DMPO and (B) POBN.

the Fenton reaction. The result indicates that instead of directly trapping ·OH, this method actually traps and measures ·CH_3 that is formed during the interaction of DMSO with ·OH. Moreover, this method could detect ·OH, which is not affected by copper ion (Fig. 3).

3.3. Measurement of hydroxyl radical by ESR using POBN as spin trapping reagent

In order to quantify DNA damage induced by phenolic compounds and copper ion, ESR analysis was conducted to determine ·OH. Fig. 5 shows that no POBN–CH_3 signal is detected in solutions containing no CaA or ChA, and that the POBN–CH_3 signal intensity was increased by the interaction of CaA or ChA with Cu^{2+}. Moreover, POBN–CH_3 signal intensity decreased when CaA or ChA concentration was increased further.

The formation of Cu^{2+} chelate with phenolic compounds was confirmed in the reaction with EDTA, a well-known chelating reagent for metal ions. Bathocuproinedisulfonic acid (a specific Cu^{+} chelator) and catalase (H_2O_2 scavenger) decreased ·OH generation induced by phenolic compounds in the presence of Cu^{2+} (Fig. 6).

In addition, the pro-oxidant activities of the interaction between phenolic compounds and copper are shown in Fig. 7. ROS was not detected without Cu^{2+} for the phenolic compounds alone. However, the results indicate that CaA, ChA, Que and catechin groups generated ROS in the presence of Cu^{2+}. Catechin groups that possessed gallate groups showed decreased pro-oxidant activity. On the other hand, FA, QA, and Res were either very small or not generated ROS at all in the presence of Cu^{2+}.

3.4. Oxidative damage and formation of 8-OHdG in calf thymus DNA

The hydroxylation of dG to form 8-OHdG adduct is an important biomarker of oxidative DNA damage. When calf thymus DNA was treated with phenolic compounds in the presence of $CuSO_4$, 8-OHdG was effectively formed. Using the same ESR conditions, we examined the effect of phenolic compounds on the copper-dependent 8-OHdG formation. Phenolic compounds alone were not increased 8-OHdG without Cu^{2+}. Catechin groups considerably increased 8-OHdG levels in DNA treated with phenolic compounds/copper (Fig. 8). Particularly, *ortho*-dihydroxyl groups that can chelate with Cu^{2+} induce the greatest pro-oxidant activity. Other compounds such as FA, QA, and Res cannot be oxidized DNA by Cu^{2+}.

4. Discussion

Phenolic compounds are widely studied for their antioxidant activity. Antioxidant activity refers to both the ability of phenolic compounds to prevent damage from ROS (through radical scavenging) and/or to prevent generation of ROS (by binding metal ion). All the phenolic compounds in our experiments showed antioxidant activity. Meanwhile, the scavenging activities of catechin and its related compounds were significantly different. It was said that the pyrogallol structure in the B-ring play an important role in the rapid scavenging ability (Kondo et al., 2001). The presence of C-ring a gallate group and/or B-ring a pyrogallol group in their structures increased their ability to scavenge free radicals (Fig. 1).

On the other hand, if phenolic compounds and copper were absorbed by the body, they would interact with each other to generate ROS. There are several reports indicating that various phenolic compounds, such as resveratrol and catechin, promote DNA damage by Cu^{2+}. Most of the reports assessed DNA damage by analyzing plasmid DNA strand breaks. This method is widely used as a model system to induce DNA strand breaks. We clearly saw the effects of ROS on DNA but could not quantify the amount of ROS produced. One study that estimated the production of ROS and/or the pro-oxidant activity used 2′,7′-dichlorodihydrofluorescein diacetate (DCFH-DA) (Labieniec and Gabryelak, 2007). Fluorogenic

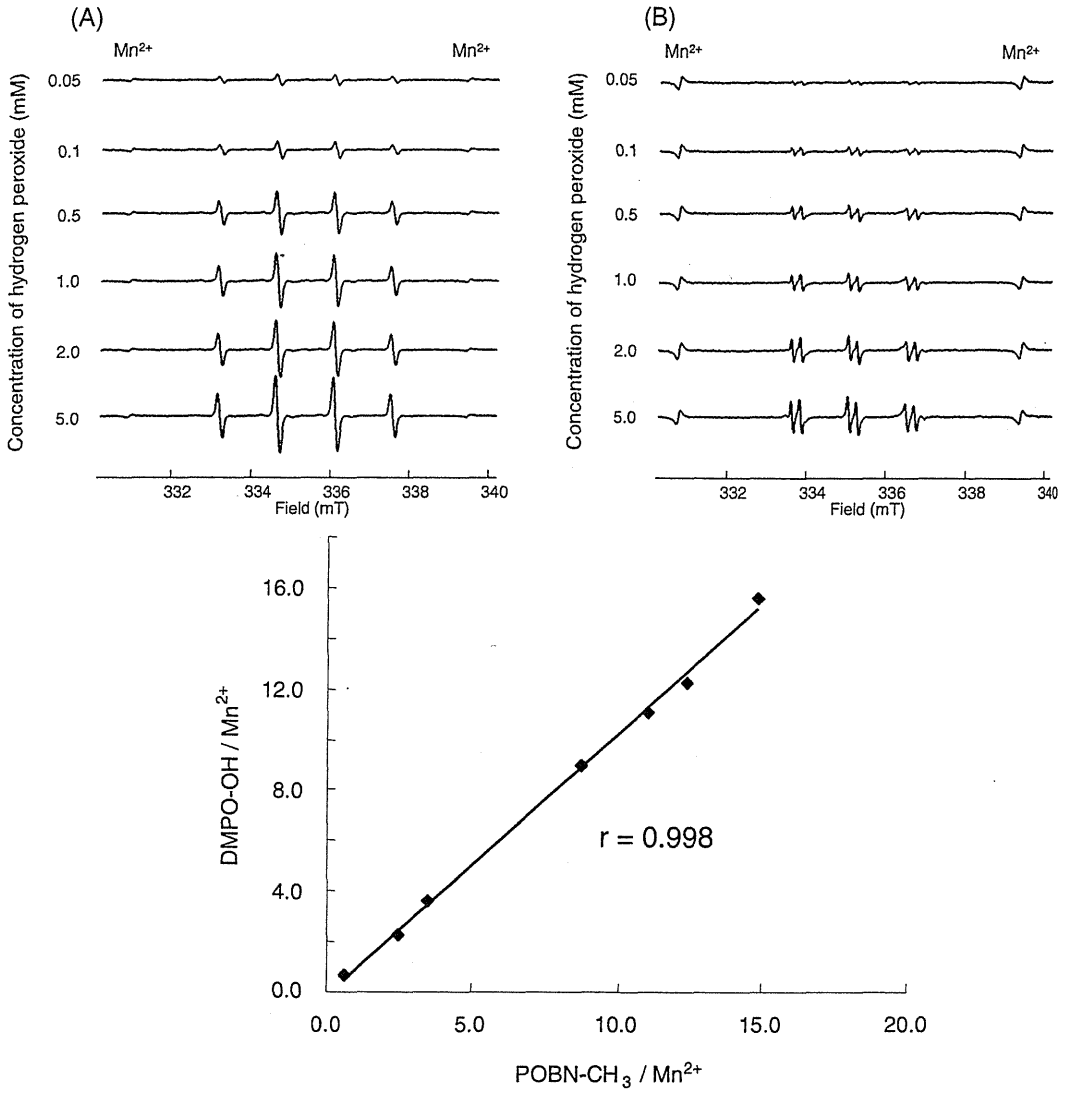

Fig. 4. Comparison of ESR spectra between (A) DMPO–OH and (B) POBN–CH_3. Correlation of DMPO–OH and POBN–CH_3 signal.

probes are widely employed to monitor oxidative activity in cells. DCFH-DA is converted into DCFH by intracellular esterases, and the non-fluorescent DCFH is oxidized to DCF by reacting with ROS. Specifically, the oxidation of DCFH is a result of the reaction with H_2O_2 or peroxynitrite (Rota et al., 1999). Although there remain many controversies particularly about the specificity, $DCFH_2$-DA/$DCFH_2$ are useful probes for oxidative studies in cell-free and biological systems. However, the oxidation of $DCFH_2$ is non-specific (Chen et al., 2010). For this reason, ROS assessment should be carefully conducted to avoid misinterpretation of results.

Free radicals have unpaired electrons that can be detected selectively by ESR measurement. The spin trapping method takes advantage of the rapid reaction of many radicals with certain chemical acceptor molecules (spin trapping reagents) to produce more stable secondary radicals. Spin trapping reagents are diamagnetic compounds that rapidly scavenge transient radicals to form stable paramagnetic spin adduct radicals. Because this secondary radical retains an unpaired electron, it can often be detected by ESR measurement. Many spin trapping reagents are available. One example is DMPO, which has been used for decades to trap oxygen radicals in biological systems. However, the use of the spin trapping technique for direct measurements in functioning biological systems is limited by the poor stability of the spin trapped adducts. On the other hand, POBN and α-phenyl-*N*-*tert*-butyl nitrone (PBN), which are nitrone spin reagents, are frequently used in *in vivo* and *in vitro* studies (Awasthi et al., 1997; Yue Qian et al., 2005) because stable adducts with carbon-centered radicals are formed. In this study, we were able to measure ROS production and pro-oxidant activity using POBN reagent instead of DMPO reagent (Fig. 4).

Phenolic compounds can switch from antioxidants to pro-oxidants in the presence of Cu^{2+} to induce ROS production and subsequently DNA damage. There are several reports that clarify the mechanism of the pro-oxidant activity. Phenolic compounds can reduce Cu^{2+} to Cu^{+} via electron transfer. In addition, chelated and/or free Cu^{+} can be oxidized to Cu^{2+}. It is said that *ortho*-dihydroxyl groups that can chelate with Cu^{2+} induce the greatest pro-oxidant activity. Actually, our results also indicated the possible mechanisms of ROS production induced by phenolic compounds in the presence of Cu^{2+}. Other compounds such as FA, QA, and Res cannot be induced ROS by Cu^{2+}, because they have no *ortho*-dihydroxyl groups. Moreover, the interaction between phenolic

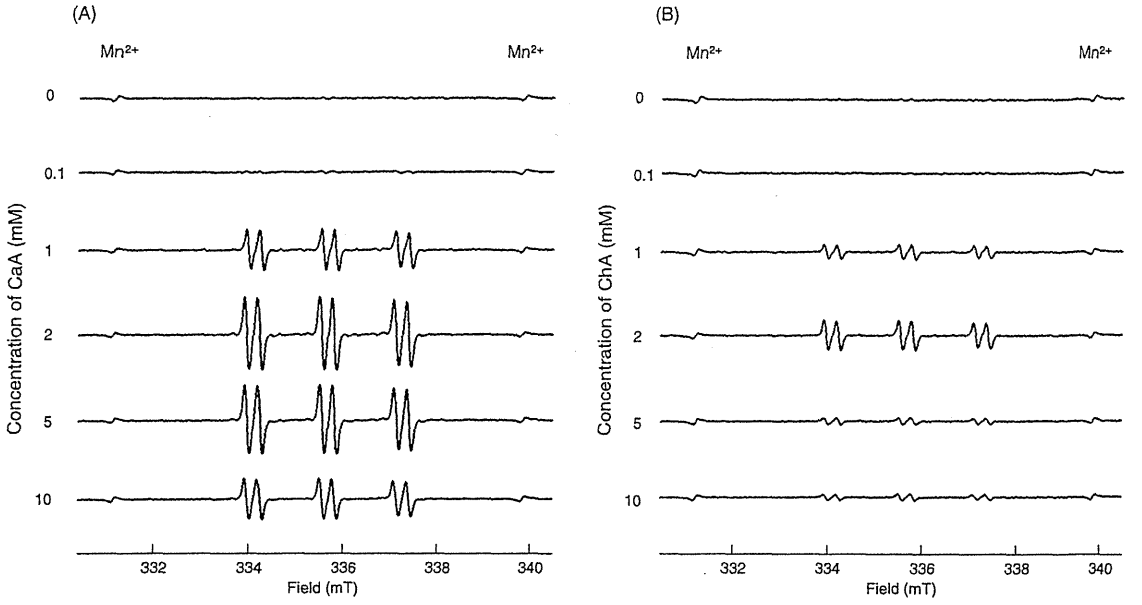

Fig. 5. Representative ESR spectra of the interaction between CaA (A) or ChA (B) and copper.The reaction mixture consisted of copper (1 mM), phenolic compound, DMSO (10%), and POBN (10 mM) in phosphate buffer (50 mM, pH 7.4), and the ESR spectra were recorded after reacting for 30 min at 37 °C.

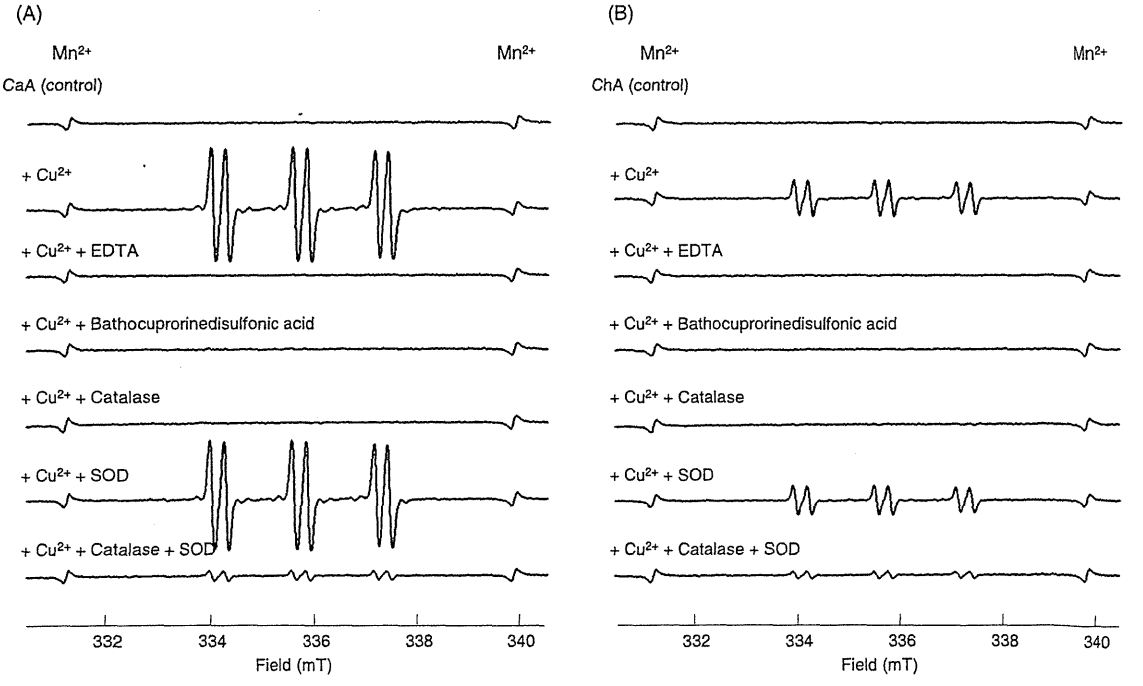

Fig. 6. Effect of chelator and antioxidant enzyme on ROS generation. The reaction mixture consisted of copper (1 mM), phenolic compound (2 mM), DMSO (10%), and POBN (10 mM) in phosphate buffer (50 mM, pH 7.4), and the ESR spectra were recorded after reacting for 30 min at 37 °C.

compounds and copper induced to H_2O_2 (Fig. 6). Both O_2 uptake and ·OH formation were suppressed by the Cu^+ chelator bathocuproine and catalase, confirming the involvement of Cu^+ and H_2O_2 in a metal catalyzed Fenton reaction. In addition, these ESR results were correlated with 8-OHdG that is effectively formed for the assessment of oxidative damage (Figs. 7 and 8).

In conclusion, we conducted ESR measurement for the increase in ROS in relation to its structure and interaction with transition metals. Moreover, we demonstrated that ROS participated in oxidative DNA damage induced by phenolic compounds in the presence of Cu^{2+}. The obtained results indicate one possibility *in vitro*. However, they are not sufficient evidence to claim that phenolic compounds are dangerous. Oral and intravenous dosing experiments revealed that phenolic compounds, such as catechin, had very low bioavailability. According to Manach et al., (2004), important inter-individual differences in the capacity to metabolize phenolic compounds originate from differences in the activities of cytochrome P450 and carrier systems that may be influenced by

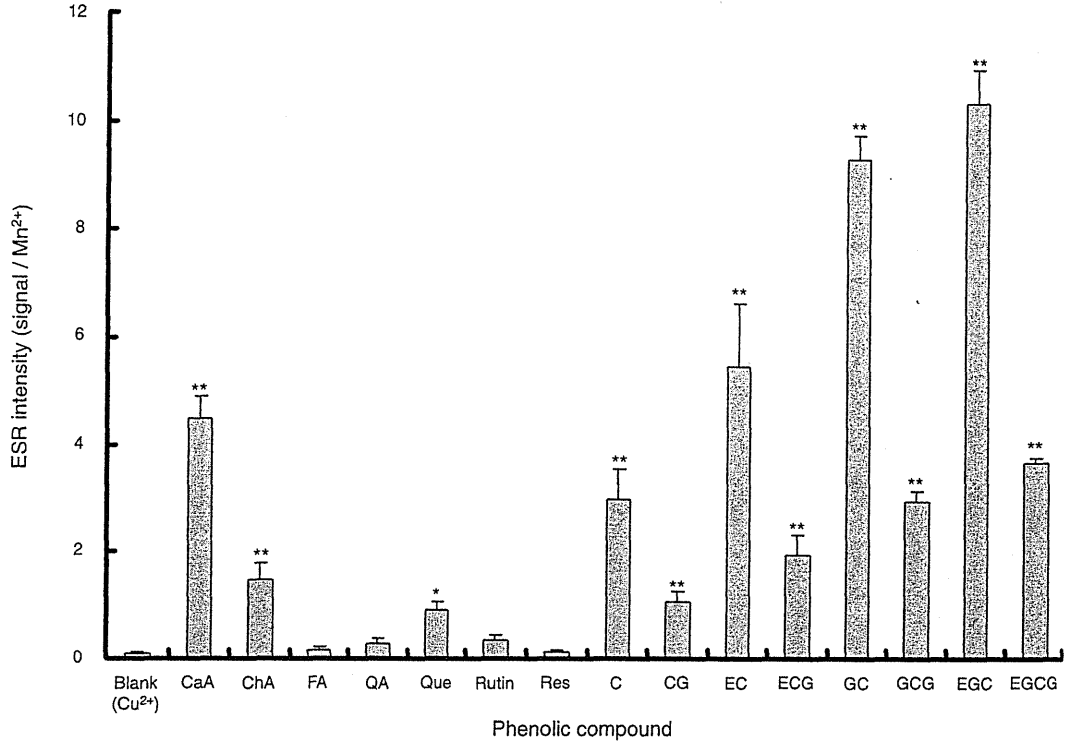

Fig. 7. Pro-oxidant activities in the interaction between phenolic compounds and copper. The concentration of each phenolic compound was 2 mM and copper concentration was 1 mM. Data points represent means ± SD ($n = 6$). * and **: statistically significant vs blank ($P < 0.05$ and $P < 0.01$ by ANOVA). CaA, caffeic acid; ChA, chlorogenic acid; FA, ferulic acid; QA, quinic acid; Que, quercetin; Res, resveratrol; C, catechin; CG, catechin gallate; EC, epicatechin; ECG, epicatechin gallate; GC, gallocatechin; GCG, gallocatechin gallate; EGC, epigallocatechin; EGCG, epigallocatechin gallate.

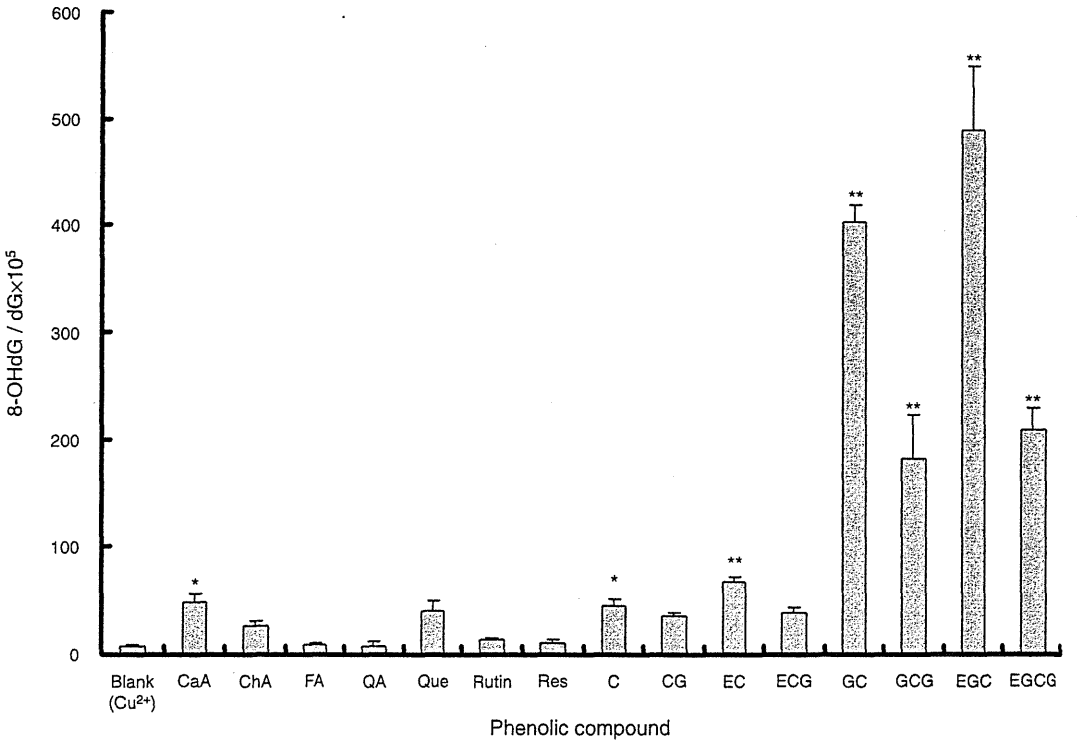

Fig. 8. Changes of 8-OHdG levels in the interaction between phenolic compounds and copper. The concentration of each phenolic compound was 0.2 mM and copper concentration was 0.1 mM. Data points represent means ± SD ($n = 6$). * and **: statistically significant vs blank ($P < 0.05$ and $P < 0.01$ by ANOVA). CaA, caffeic acid; ChA, chlorogenic acid; FA, ferulic acid; QA, quinic acid; Que, quercetin; Res, resveratrol; C, catechin; CG, catechin gallate; EC, epicatechin; ECG, epicatechin gallate; GC, gallocatechin; GCG, gallocatechin gallate; EGC, epigallocatechin; EGCG, epigallocatechin gallate.

genetic polymorphisms. In contrast to the pharmacokinetic profiles of flavonoids, such as catechin (Masukawa et al., 2006) and isoflavones (Pascual-Teresa et al., 2006), various plasma concentration peaks were observed from 0.5 h to 8 h after the consumption of green coffee extract, suggesting a complex and dynamic process underlying absorption and metabolism (Farah et al., 2008). Therefore, it seems reasonable to conclude that the most important consideration is the disturbance of the pro-oxidant/antioxidant system in favor of the former. Further studies are required to reveal the chemical mechanisms of the antioxidant activity and the pro-oxidant activity of phenolic compounds.

Acknowledgement

This work was supported by a Grant-in-Aid from the Ministry of Health, Labour and Welfare, Japan.

References

Ahmad, A., Syed, F.A., Singh, S., Hadi, S.M., 2005. Prooxidant activity of resveratrol in the presence of copper ions: mutagenicity in plasmid DNA. Toxicol. Lett. 159, 1–12.

Ahsan, H., Hadi, S.M., 1998. Strand scission in DNA induced by curcumin in the presence of Cu(II). Cancer Lett. 124, 23–30.

Al-Ebraheem, A., Farquharson, M.J., Ryan, E., 2009. The evaluation of biologically important trace metals in liver, kidney and breast tissue. Appl. Radiat. Isot. 67, 470–474.

Awasthi, D., Church, D.F., Torbati, D., Carey, M.E., Pryor, W.A., 1997. Oxidative stress following traumatic brain injury in rats. Surg. Neurol. 47, 575–581.

Babbs, C.F., Steiner, M.G., 1990. Detection and quantitation of hydroxyl radical using dimethyl sulfoxide as molecular probe. Methods Enzymol. 186, 137–147.

Barr, D.P., Martin, M.V., Guengerich, F.P., Mason, R.P., 1996. Reaction of cytochrome P450 with cumene hydroperoxide: ESR spin-trapping evidence for the homolytic scission of the peroxide O–O bond by ferric cytochrome P450 1A2. Chem. Res. Toxicol. 9, 318–325.

Bjelakovic, G., Nikolova, D., Gluud, L.L., Simonetti, R.G., Gluud, C., 2007. Mortality in randomized trials of antioxidant supplements for primary and secondary prevention: systematic review and meta-analysis. JAMA 297, 842–857.

Cabrera, C., Artacho, R., Giménez, R., 2006. Beneficial effects of green tea – a review. J. Am Coll. Nutr. 25, 79–99.

Cao, G., Sofic, E., Prior, R.L., 1997. Antioxidant and prooxidant behavior of flavonoids: structure–activity relationships. Free Radic. Biol. Med. 22, 749–760.

Chen, X., Zhong, Z., Xu, Z., Chen, L., Wang, Y., 2010. 2′,7′-Dichlorodihydrofluorescein as a fluorescent probe for reactive oxygen species measurement: forty years of application and controversy. Free Radic. Res. 44, 587–604.

Del Carlo, M., Sacchetti, G., Di Mattia, C., Compagnone, D., Mastrocola, D., Liberatore, L., Cichelli, A., 2004. Contribution of the phenolic fraction to the antioxidant activity and oxidative stability of olive oil. J. Agric. Food Chem. 52, 4072–4079.

Fan, G.J., Jin, X.L., Qian, Y.P., Wang, Q., Yang, R.T., Dai, F., Tang, J.J., Shang, Y.J., Cheng, L.X., Yang, J., Zhou, B., 2009. Hydroxycinnamic acids as DNA-cleaving agents in the presence of Cu(II) ions: mechanism, structure–activity relationship, and biological implications. Chemistry 15, 12889–12899.

Farah, A., Monteiro, M., Donangelo, C.M., Lafay, S., 2008. Chlorogenic acids from green coffee extract are highly bioavailable in humans. J. Nutr. 138, 2309–2315.

Gardner, E.J., Ruxton, C.H., Leeds, A.R., 2007. Black tea-helpful or harmful? A review of the evidence. Eur. J. Clin. Nutr. 61, 3–18.

Hayakawa, F., Kimura, T., Maeda, T., Fujita, M., Sohmiya, H., Fujii, M., Ando, T., 1997. DNA cleavage reaction and linoleic acid peroxidation induced by tea catechins in the presence of cupric ion. Biochim. Biophys. Acta 1336, 123–131.

Ishii, Y., Ogara, A., Okamura, T., Umemura, T., Nishikawa, A., Iwasaki, Y., Ito, R., Saito, K., Hirose, M., Nakazawa, H., 2007. Development of quantitative analysis of 8-nitroguanine concomitant with 8-hydroxydeoxyguanosine formation by liquid chromatography with mass spectrometry and glyoxal derivatization. J. Pharm. Biomed. Anal. 43, 1737–1743.

Jung, Y., Surh, Y., 2001. Oxidative DNA damage and cytotoxicity induced by copper-stimulated redox cycling of salsolinol, a neurotoxic tetrahydroisoquinoline alkaloid. Free Radic. Biol. Med. 30, 1407–1417.

Kagawa, T.F., Geierstanger, B.H., Wang, A.H., Ho, P.S., 1991. Covalent modification of guanine bases in double-stranded DNA. The 1.2-A Z-DNA structure of d(CGCGCG) in the presence of $CuCl_2$. J. Biol. Chem 266, 20175–20184.

Kanabrocki, E.L., Sothern, R.B., Ryan, M.D., Kahn, S., Augustine, G., Johnson, C., Foley, S., Gathing, A., Eastman, G., Friedman, N., Nemchausky, B.A., Kaplan, E., 2008. Circadian characteristics of serum calcium, magnesium and eight trace elements and of their metallo-moieties in urine of healthy middle-aged men. Clin. Ter. 159, 329–346.

Kondo, K., Kurihara, M., Fukuhara, K., 2001. Mechanism of antioxidant effect of catechins. Methods Enzymol. 335, 203–217.

Labieniec, M., Gabryelak, T., 2007. Antioxidative and oxidative changes in the digestive gland cells of freshwater mussels Unio tumidus caused by selected phenolic compounds in the presence of H_2O_2 or Cu^{2+} ions. Toxicol. In Vitro 21, 146–156.

Lodovici, M., Guglielmi, F., Casalini, C., Meoni, M., Cheynier, V., Dolara, P., 2001. Antioxidant and radical scavenging properties in vitro of polyphenolic extracts from red wine. Eur. J. Nutr. 40, 74–77.

Makris, D.P., Psarra, E., Kallithraka, S., Kefalas, P., 2003. The effect of polyphenolic composition as related to antioxidant capacity in white wines. Food Res. Int. 36, 805–814.

Manach, C., Scalbert, S., Morand, C., Rémésy, C., Jiménez, L., 2004. Polyphenols: food sources and bioavailability. Am. J. Clin. Nutr. 79, 727–747.

Masukawa, Y., Matsui, Y., Shimizu, N., Kondou, N., Endou, N., Kuzukawa, M., Hase, T., 2006. Determination of green tea catechins in human plasma using liquid chromatography-electrospray ionization mass spectrometry. J. Chromatogr. B: Analyt. Technol. Biomed. Life Sci. 834, 26–34.

Nardini, M., Cirillo, E., Natella, F., Scaccini, C., 2002. Absorption of phenolic acids in humans after coffee consumption. J. Agric. Food Chem. 50, 5735–5741.

Pascual-Teresa, S.T., Hallund, J., Talbot, D., Schroot, J., Williams, C.M., Bugel, S., Cassidy, A., 2006. Absorption of isoflavones in humans: effects of food matrix and processing. J. Nutr. Bioch. 17, 257–264.

Perron, N.R., Brumaghim, J.L., 2009. A review of the antioxidant mechanisms of polyphenol compounds related to iron binding. Cell Biochem. Biophys. 53, 75–100.

Rico, H., Roca-Botran, C., Hernández, E.R., Seco, C., Paez, E., Valencia, M.J., Villa, L.F., 2000. The effect of supplemental copper on osteopenia induced by ovariectomy in rats. Menopause 7, 413–416.

Rota, C., Chignell, C.F., Mason, R.P., 1999. Evidence for free radical formation during the oxidation of 2′-7′-dichlorofluorescin to the fluorescent dye 2′-7′-dichlorofluorescein by horseradish peroxidase: Possible implications for oxidative stress measurements. Free Radic. Biol. Med. 27, 873–881.

Sugihara, N., Arakawa, T., Ohnishi, M., Furuno, K., 1999. Anti- and pro-oxidative effects of flavonoids on metal-induced lipid hydroperoxide-dependent lipid peroxidation in cultured hepatocytes loaded with alpha-linolenic acid. Free Radic. Biol. Med. 27, 1313–1323.

Szydłowska-Czerniak, A., Trokowski, K., Karlovits, G., Szłyk, E., 2010. Determination of antioxidant capacity, phenolic acids, and fatty acid composition of rapeseed varieties. J. Agric. Food Chem. 58, 7502–7509.

Vinson, J.A., Hao, Y., Su, X., Zubik, L., 1998. Phenol antioxidant quantity and quality in foods: vegetables. J. Agric. Food Chem. 46, 3630–3634.

Vinson, J.A., Su, X., Zubik, L., Bose, P., 2001. Phenol antioxidant quantity and quality in foods: fruits. J. Agric. Food Chem. 49, 5315–5321.

Wang, T., Chen, L.X., Long, Y., Wu, W.M., Wang, R., 2008. DNA damage induced by caffeic acid phenyl ester in the presence of Cu(II) ions: potential mechanism of its anticancer properties. Cancer Lett. 263, 77–88.

Yamashita, N., Tanemura, H., Kawanishi, S., 1999. Mechanism of oxidative DNA damage induced by quercetin in the presence of Cu(II). Mutat. Res. 425, 107–115.

Yao, L.H., Jiang, Y.M., Shi, J., Tomás-Barberán, F.A., Datta, N., Singanusong, R., Chen, S.S., 2004. Flavonoids in food and their health benefits. Plant Foods Hum. Nutr. 59, 113–122.

Yue Qian, S., Kadiiska, M.B., Guo, Q., Mason, R.P., 2005. A novel protocol to identify and quantify all spin trapped free radicals from in vitro/in vivo interaction of HO· and DMSO: LC/ESR, LC/MS, and dual spin trapping combinations. Free Radic. Biol. Med. 38, 125–135.

Zheng, L.F., Wei, Q.Y., Cai, Y.J., Fang, J.G., Zhou, B., Yang, L., Liu, Z.L., 2006. DNA damage induced by resveratrol and its synthetic analogues in the presence of Cu (II) ions: mechanism and structure–activity relationship. Free Radic. Biol. Med. 41, 1807–1816.

Zheng, L.F., Dai, F., Zhou, B., Yang, L., Liu, Z.L., 2008. Prooxidant activity of hydroxycinnamic acids on DNA damage in the presence of Cu(II) ions: mechanism and structure–activity relationship. Food Chem. Toxicol. 46, 149–156.

Archives of Biochemistry and Biophysics 513 (2011) 10–18

Contents lists available at ScienceDirect

Archives of Biochemistry and Biophysics

journal homepage: www.elsevier.com/locate/yabbi

Characterization of nitrated phenolic compounds for their anti-oxidant, pro-oxidant, and nitration activities

Yusuke Iwasaki [a,*], Maki Nomoto [a], Momoko Oda [a], Keisuke Mochizuki [a], Yuki Nakano [a], Yuji Ishii [b], Rie Ito [a], Koichi Saito [a], Takashi Umemura [b], Akiyoshi Nishikawa [b], Hiroyuki Nakazawa [a]

[a] Department of Analytical Chemistry, Faculty of Pharmaceutical Sciences, Hoshi University, 2-4-41 Ebara, Shinagawa-ku, Tokyo 142-8501, Japan
[b] Division of Pathology, National Institute of Health Sciences, 1-18-1 Kamiyoga, Setagaya-ku, Tokyo 158-8501, Japan

ARTICLE INFO

Article history:
Received 11 May 2011
and in revised form 15 June 2011
Available online 24 June 2011

Keywords:
Chlorogenic acid
Caffeic acid
Sodium nitrite
Anti-oxidant
Pro-oxidant

ABSTRACT

Coffee is one of the most widely consumed beverages worldwide. Evidence of the health benefits and the important contribution of coffee brew to the intake of anti-oxidants in the diet has increased coffee consumption. Chlorogenic acid (ChA) and caffeic acid (CaA) are the major phenolic compounds in coffee. However, phenolic compounds, which are generally effective anti-oxidants, can become pro-oxidants in the presence of Cu^{2+} to induce DNA damage under certain conditions. On the other hand, sodium nitrite ($NaNO_2$) is widely used as a food additive to preserve and tinge color on cured meat and fish. It is possible that phenolic compounds react with $NaNO_2$ under acidic conditions, such as gastric juice. In this study, we identified compounds produced by the reaction between ChA or CaA in coffee and $NaNO_2$ in artificial gastric juice. The identified phenolic compounds and nitrated phenolic compounds were assessed for their anti-oxidant, pro-oxidant, and nitration activities by performing an *in vitro* assay. The nitrated phenolic compounds seemed to show increased anti-oxidant activity and decreased pro-oxidant activity. However, one nitrated CaA compound that has a furoxan ring showed the ability to release NO_2^- in the neutral condition.

Introduction

Coffee is one of the most widely consumed beverages worldwide. During the past few years, evidence of the health benefits [1] and the important contribution of coffee brew to the intake of anti-oxidants in the diet [2–4] has increased coffee consumption. Many studies have examined the association between coffee consumption and health, particularly cardiovascular morbidity. The question of whether or not coffee intake increases the risk of coronary heart disease remains unanswered. Several studies have shown that caffeine in coffee induces various acute cardiovascular effects, including effects on blood pressure, circulating catecholamines, arterial stiffness, and endothelium-dependent vasodilation [5,6]. On the other hand, coffee consumption is also associated with the decreased risk of type 2 diabetes [7], Alzheimer's disease [8], and cancer [9]. It is said that these effects are produced by polyphenols, which have anti-oxidant activity. Anti-oxidant activity refers to the ability of polyphenol compounds to prevent damage caused by reactive oxygen species (ROS) (such as by radical scavenging) or to prevent the generation of these species (by binding iron) [10]. Chlorogenic acid (ChA) and caffeic acid (CaA) are the major phenolic compounds in coffee and act as anti-oxidants. However, phenolic compounds, which are generally effective anti-oxidants, can become pro-oxidants in the presence of Cu^{2+} to induce DNA damage under certain conditions. It has been demonstrated that compounds bearing *o*-dihydroxyl groups (i.e., ChA and CaA) are the most active in inducing plasmid pBR322 DNA strand breakage in the presence of Cu^{2+} [11].

The major dietary source of nitrite includes cured meat and cereals, but approximately 90% of nitrite ingested by humans is accounted for by the reduction of nitrate in the oral cavity via the action of nitrate reductase produced by microorganisms present in the oral cavity [12]. Sodium nitrite ($NaNO_2$) is widely used as a food additive to preserve and tinge color on cured meat and fish [13]. Nitrite concentrations *in vivo* are 0.5–3.6 μM in plasma [14], 15 μM in respiratory tract lining fluid [15], and 30–210 μM in saliva [16], making nitrous acid formation likely in many tissue compartments. Excessive nitrite production is noted particularly in inflammation. Humans, therefore, ingest nitrite from both exogenous and endogenous sources. At the acidic pH of the stomach, nitrite yields nitric oxide (NO) and NO-derived species that may exert a biological impact locally in terms of antimicrobial effects, blood flow, mucus secretion, and gastric motility. It has been reported that the co-administration of catechol and $NaNO_2$ to rats increased 8-hydroxy-2′-deoxyguanosine (8-OHdG) levels in forestomach epithelium DNA [17].

* Corresponding author. Fax: +81 3 5498 5765.
E-mail address: iwasaki@hoshi.ac.jp (Y. Iwasaki).

0003-9861/$ - see front matter © 2011 Elsevier Inc. All rights reserved.
doi:10.1016/j.abb.2011.06.009

Some dietary phenolics with anti-oxidant activity can reduce nitrite to NO under acidic conditions. As coffee contains ChA and CaA, it is possible that these compounds reduce nitrous acid to NO when $NaNO_2$ is mixed with gastric juice after drinking coffee. In fact, it has been reported that ChA and CaA were nitrated by $NaNO_2$ under acidic conditions, and the nitration could give rise to several nitrated ChA and CaA compounds *in vitro* [18]. However, there are no reports of the characteristics of the nitrated compounds.

In the present study, we identified compounds produced by the reaction between ChA or CaA in coffee and $NaNO_2$ in artificial gastric juice. The identified phenolic compounds and the nitrated phenolic compounds were assessed for their anti-oxidant, pro-oxidant, and nitration activities by performing an *in vitro* assay.

Materials and methods

Reagents and chemicals

Chlorogenic acid (ChA) was purchased from Tokyo Chemical Industry (Tokyo, Japan). Caffeic acid (CaA), nuclease P1, and DNA Extractor Kit were purchased from Wako Pure Chemical Industries (Tokyo, Japan). Copper(II) sulfate pentahydrate and sodium nitrite ($NaNO_2$) were purchased from Kanto Chemical (Tokyo, Japan). α-(4-Pyridyl-1-oxide)-*N*-*tert*-butylnitrone (POBN) was purchased from Labotech Co. (Tokyo, Japan). Deoxyribonucleic acid sodium salt from calf thymus, phosphatase alkaline from bovine intestinal mucosa, deoxyguanosine (dG), and 8-hydroxy-2′-deoxyguanosine (8-OHdG) were obtained from Sigma (Tokyo, Japan). Water was purified using a Milli-Q gradient A10 system (Millipore, MA, USA). Other chemicals and solvents were obtained from Wako Pure Chemical Industries.

Synthesis of nitrated chlorogenic acid and caffeic acid

Nitrated ChA and CaA were synthesized according to the method reported by Napolitano and d'Ischia [18]. Briefly, ChA or CaA (5 mmol) was dissolved in 0.05 M acetate buffer, pH 4 (500 mL) and $NaNO_2$ (25 mmol) and the mixture was continuously stirred at room temperature. Then, the mixture was extracted with ethyl acetate (3 × 150 mL) and the combined organic layers were dried over sodium sulfate to dryness. The target substance was removed from the reaction solution by silica gel chromatography using toluene–ethyl acetate 80:20 (eluent A), 60:40 (eluent B) or 40:60 (eluent C). Purified nitrated ChA and CaA were identified by comparison of their spectral properties (^1H NMR, ^{13}C NMR, and LC-PDA-ESI-MS) with those reported [18,19]. Their chemical structures are shown in Fig. 1.

Nitrochlorogenic acid (ChA-NO). UV: λ_{max} (MeOH) 276, 339, 430 nm. ^1H NMR (CD_3OD) δ (ppm): 2.12 (m, 4H), 3.74 (dd, J = 10.0, 3.2 Hz, 1H), 4.20 (m, 1H), 5.42 (m, 1H), 6.31 (d, J = 15.6 Hz, 1H), 7.05 (s, 1H), 7.57 (s, 1H), 8.15 (d, J = 15.6 Hz, 1H).

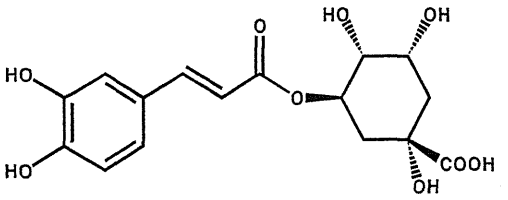

Chlorogenic acid (ChA)

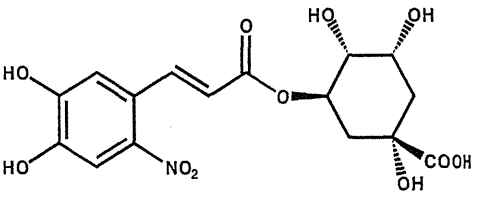

Nitrochlorogenic acid
(ChA-NO)

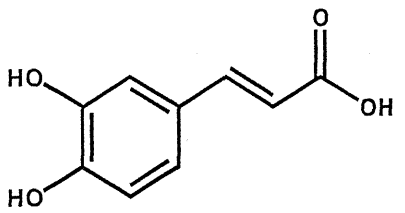

Caffeic acid (CaA)

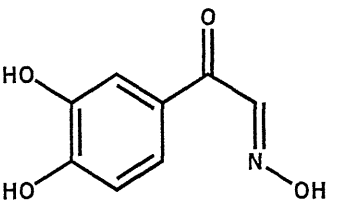

2-(3,4-Dihydroxyphenyl)-2-oxoethanaloxime
(CaA-NO-1)

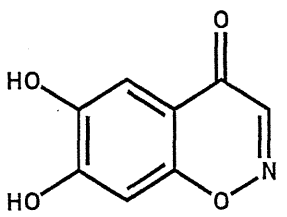

6,7-Dihydroxy-1,2-(4*H*)-benzoxazin-4-one
(CaA-NO-2)

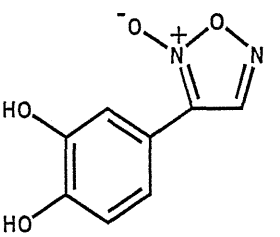

2-Oxy-3-(3,4-dihydroxyphenyl)-1,2,5-oxadiazole
(CaA-NO-3)

Fig. 1. Structures of ChA, CaA, and nitrated phenolic compounds.

^{13}C NMR (CD_3OD) δ (ppm): 39.5 (CH_2), 41.3 (CH_2), 73.2 (CH), 73.3 (CH), 75.3 (C), 78.2 (CH), 113.2 (CH), 116.0 (CH), 121.2 (CH), 125.6 (C), 140.7 (C), 144.0 (CH), 150.2 (C), 156.2 (C), 169.1 (C), 181.8 (C). ESI-MS: *m/z* 398 $[M-H]^-$.

2-(3,4-Dihydroxyphenyl)-2-oxoethanaloxime (CaA-NO-1). ^{1}H NMR (acetone-d_6) δ (ppm): 6.91 (d, 1 H, J = 8.8 Hz), 7.61 (dd, 1H, J = 8.8, 2.0 Hz), 7.62 (d, 1H, J = 2.0 Hz), 7.91 (s, 1H). ^{13}C NMR (acetone-d_6) δ (ppm): 115.2 (CH), 117.1 (CH), 124.5 (CH), 129.2 (C), 141.7 (C), 145.3 (C), 148.7 (CH), 187.1 (C). ESI-MS: *m/z* 180 $[M-H]^-$.

6,7-Dihydroxy-1,2-(4H)-benzoxazin-4-one (CaA-NO-2). ^{1}H NMR (CD_3OD) δ (ppm): 6.95 (s, 1H), 7.33 (s, 1H), 8.13 (s, 1H). ESI-MS: *m/z* 178 $[M-H]^-$.

2-Oxy-3-(3,4-dihydroxyphenyl)-1,2,5-oxadiazole (CaA-NO-3). UV: λ_{max} (CH_3OH) 247, 316 nm. ^{1}H NMR (CD_3OD) δ (ppm): 6.89 (d, J = 8.4 Hz, 1H), 7.32 (dd, J = 8.4, 2.0 Hz, 1H), 7.54 (d, J = 2.0 Hz, 1H), 8.92 (s, 1H). ^{13}C NMR δ (ppm): 113.9 (CH), 115.4 (C), 116.2 (C), 117.3 (CH), 120.1 (CH), 146.4 (CH), 147.5 (C), 149.7 (C). ESI-MS: *m/z* 193 $[M-H]^-$.

Analytical conditions for ChA, CaA, and nitrated phenolic compounds

High-performance liquid chromatography was performed with a SHIMADZU (Shimadzu, Tokyo, Japan) system that consisted of an LC-10AD$_{VP}$ pump, an SIL-HTC autosampler, a CTO-10A$_{VP}$ thermostated column compartment, a DGU-14AM vacuum degasser, and a SPD-M10A$_{VP}$ photodiode array detector, and was connected to a SHIMADZU LCMS-2010 A mass spectrometer. Separation of the analytes was accomplished on an Xbridge C18 column (3.5 μm, 2.1 × 150 mm; Waters, Japan). Column oven temperature was maintained at 40 °C. Mobile phase was 0.1% aqueous formic acid and 0.1% formic acid in acetonitrile (90:10, v/v) and the flow rate was constant at 0.2 mL/min.

The photodiode array detector was set at 300 nm. The analytes were detected in the electrospray negative ionization mode using the scan ion monitoring mode. Curved desolvation line and heat block temperatures for the analysis were set at 250 and 200 °C, respectively. Nebulizer gas flow was set at 1.5 L/min and detector voltage was set at 1.3 eV.

DPPH radical scavenging activity

The modified DPPH method was used for the determination of anti-oxidant activity [20]. DPPH radical solution (2 mM) was prepared in methanol and the phenolic compounds were diluted in methanol to concentrations ranging from 0.1 to 2 mM. In a 1.5 mL disposable tube, the prepared DPPH (250 μL) solution was added to a sample of diluted phenolic compound (50 μL) and methanol (200 μL). The mixed samples were incubated for 30 min at 37 °C. Absorbance was monitored at 540 nm with a BIO-RAD Model 550 microplate reader. Then, the effect of phenolic compounds on DPPH· absorbance was estimated. DPPH scavenging activity was determined with the following equation: % scavenging activity = $[A_{control} - A_{sample}]/[A_{control} - A_{ascorbic\ acid}] \times 100$. DPPH plus ascorbic acid (10 mM) was used as positive control. Data are means ± SD of three determinations.

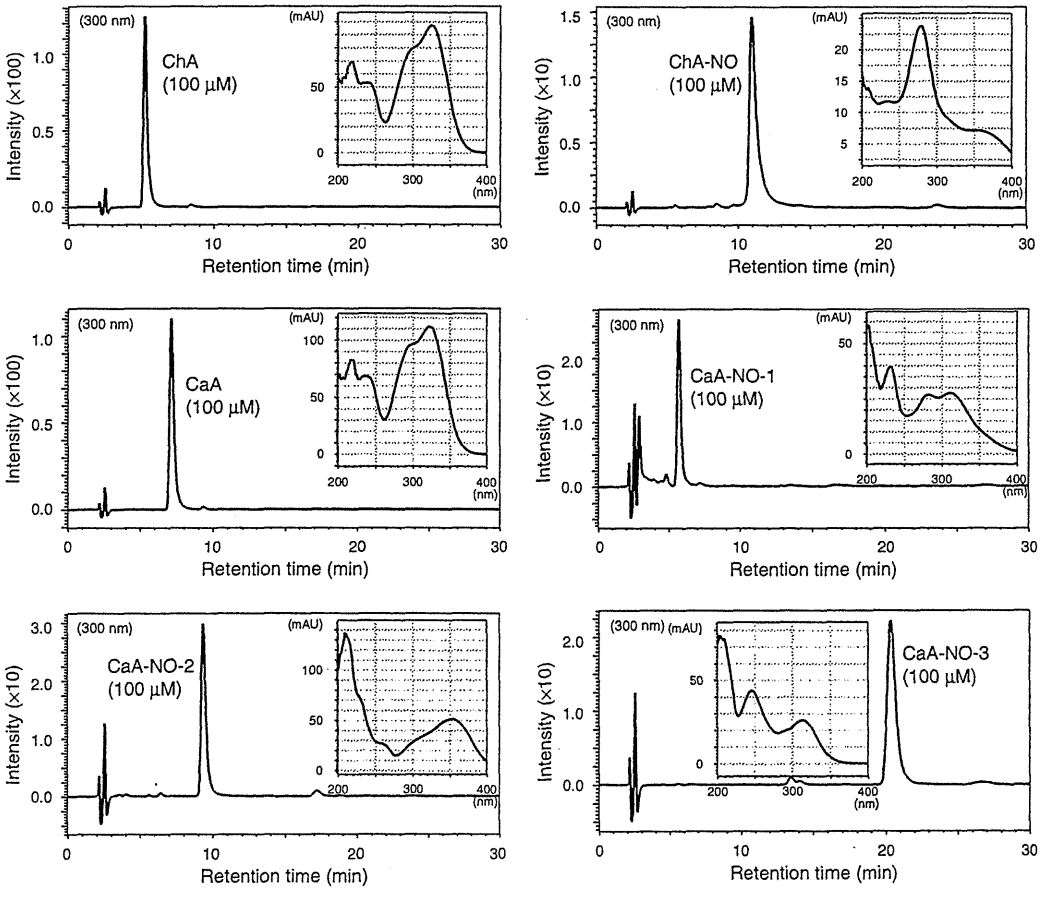

Fig. 2. UV chromatograms and spectra of ChA, CaA, and nitrated phenolic compounds. Separation of the analytes was accomplished on an XBridge C18 column (3.5 μm, 2.1 × 150 mm; Waters, Japan). Mobile phase was 0.1% aqueous formic acid and 0.1% formic acid in acetonitrile (90:10, v/v).